Generation and Fate of Glacial Sediments in the central Transantarctic Mountains based on Radiogenic Isotopes and Implications for Reconstructing Past Ice Dynamics

G. Lang Farmer, Department of Geological Sciences, University of Colorado Boulder 80309*

Kathy J. Licht, Department of Earth Sciences, Indiana University– Purdue University Indianapolis, Indianapolis, IN 46202

*corresponding author; farmer@colorado.edu

Abstract

The Nd, Sr and Pb isotopic compositions of glacial tills from the Byrd and Nimrod glaciers in the central Transantarctic Mountains (TAM) in East Antarctica were obtained to assess the sources of detritus transported by these ice masses. Tills from lateral moraines along the entire extent of both glaciers have isotopic compositions consistent with their derivation predominately from erosion of adjacent bedrock. Fine- (<63μ) and coarser-grained (0.5mm-2mm) sediment from these tills have identical isotopic characteristics, indicating that fine-grained detritus is the product of further comminution of coarser sediments. Comparison of present-day till isotopic data to existing data from fine-grained LGM tills in the central Ross Sea confirm that these were deposited from East Antarctic ice that expanded through the TAM and indicates that the LGM sediments are mixtures of detritus eroded along the entire path of ice transiting the TAM. If specific lithologies were preferentially eroded as ice passed through the TAM, it is not clearly evident in the Ross Sea till isotopic compositions Our data do demonstrate, however, that glacial tills generated from erosion of inboard regions of the mountain belt yield sediment with a larger component of 560 Ma to 600 Ma detrital zircons and lower average $\varepsilon_{Nd}(0)$ values (<-5) than that produced further downstream. As a result, past retreat of ice grounding-lines up the narrow valleys of the TAM resulting in active erosion of inboard region should recognizable in glacial sediments deposited in the Ross Sea, and so provide a means to identify times when the East Antarctic ice sheet was smaller than today. This study highlights both the value and necessity of utilizing multiple provenance methods in evaluating glacial erosion and transport when reconstructing past ice sheet dynamics.

1. Introduction

Assessing potential instabilities in the East Antarctica Ice Sheet (EAIS) during warming climatic conditions is critical given the role that the degradation of the EAIS plays in raising global sea level (Dolan, 2011). One approach is to investigate past instabilities in the EAIS, particularly during earlier warm periods such as the Mid-Pliocene (Austermann et al., 2015; Sugden, 1996; Winnick and Caves, 2015; Yokoyama et al., 2016). For this purpose, radiogenic isotope analyses (Nd, Sr, Pb) of glaciomarine sediments deposited on the continental shelf provide important insights into the behavior of the EAIS, an approach that has been successful in identifying EAIS expansion into Ross Embayment during the LGM (Farmer et al., 2006; Licht et al., 2005) and ice margin retreat along the Adélie Land coast during the Mid-Pliocene Warm Period (Cook et al., 2013). A full assessment of the potential of radiogenic isotope data in reconstructing past dynamics of the EAIS, however, is lacking and will require a better understanding of the factors that control the sources of glacial sediment delivered to and deposited at any given portion of the ice margin during both ice expansion and retreat. Is the locus of erosion and sediment production concentrated at the ice margin (Alley et al., 1997; Jamieson et al., 2010)? Do the sources of glacial sediments vary during ice expansion and retreat when the ice margin overrides a region of high underlying basement relief and focused ice flow (Creyts et al., 2014)? Even if the locus of bedrock erosion shifts as a regular function of ice extent, does the detritus produced inherit a radiogenic isotope that could be unambiguously used to assess the sediment provenance along a given portion of the EAIS margin?

In this study, we address some of the above issues through the use of radiogenic isotope data obtained principally from the <63μ size fraction of tills deposited by the Byrd and Nimrod glaciers to help determine the sources of sedimentary material generated and transported by ice currently traversing the Transantarctic Mountains (TAM). These data are used to assess the locus of erosion that produced subglacial sediments deposited in the central and western Ross Sea during the LGM, and to assess the likelihood that major retreat or expansion of the EAIS would produce changes in the

71 primary sources of EAIS-derived sediment deposited in the Ross Sea that would be
72 identifiable from radiogenic isotopic data.

73 The new and existing isotopic data from modern tills in the central TAM indicate
74 that these sediments represent the products of erosion and communition of adjacent
75 bedrocks, with downstream isotopic compositions of <63μ tills reflecting changes in the
76 age and/or lithology of local bedrocks. Tills inboard of where the Byrd and Nimrod
77 glaciers enter the TAM, in contrast, contain detritus that most likely derived from
78 otherwise unexposed Precambrian basement sources underlying adjacent portions of the
79 EAIS. When combined with existing chemical, isotopic, and zircon U-Pb age data from
80 central-western Ross Sea LGM tills, our data confirm that the LGM tills are complex
81 mixtures of detritus derived largely from glaciers traversing across the entire width of the
82 central TAM. Although the relative contributions of specific TAM bedrock contributions
83 to LGM tills cannot be unambiguously determined, our data do suggest that grounding
84 line retreat through the TAM in the past should be recognizable in both the radiogenic
85 isotopic compositions of fine-grained glaciomarine sediments and in the U-Pb ages of
86 detrital zircons delivered to the Ross Embayment during such events.

87 **2. Geologic Setting/Previous Studies**

88 This study targets tills associated with the Byrd and Nimrod glaciers in the central
89 TAM, the latter representing the two dominant sources of ice contributed by the EAIS to
90 the Ross ice shelf today (Humbert et al., 2005). The central TAM is well-suited for an
91 assessment of the production and transport of glacial till because the bedrock geology
92 varies regularly across the strike of the mountain belt, parallel to the direction of ice flow
93 of the main outlet glaciers (Fig. 1) (Elliot, 2013). Both the Byrd and Nimrod glaciers
94 channelize EAIS ice that overrode Proterozoic basement rocks prior to entering the
95 central TAM (Goodge et al., 2001; Goodge et al., 2008) and that traversed a set of
96 Phanerozoic sedimentary and igneous rocks before spilling into the Ross Ice Shelf. The
97 Byrd glacier is distinct, however, because it overlies a post 40 Ma fault zone that
98 produced ~1km of relative uplift of the southern and northern boundaries of the glacial
99 valley (Foley et al., 2013). The north side of the glacial valley is comprised of Cambro-
100 Ordovician Granite Harbor Intrusive Suite rocks that intruded high grade metamorphic

rocks of the Horney Unit (Fig. 1) (Borg et al., 1990). Detrital zircons in moraines along these outcrops are dominated by ages ~530 Ma (Licht and Palmer, 2013), consistent with bedrock ages of 531.0 ± 7.5 Ma on a diorite and 545.7 ± 6.8 Ma on a foliated granite (Stump et al., 2006). On the south side of Byrd Glacier, the bedrock is Lower Cambrian to Ordovician Shackleton Limestone, Douglas Conglomerate, Madison Marble and Contortion Schist; the latter were named the Selborne Group and subsequently determined to be equivalent to formations in the Byrd Group (Myrow et al., 2002; Stump et al., 2004). At the head of the Byrd Glacier, nunataks are composed of Devonian Beacon Supergroup siliciclastic rocks and Ferrar Supergroup dolerites (Anderson, 1979; Grindley and Laird, 1969) (Fig. 1). The age and composition of East Antarctic Precambrian basement rocks further inland within the catchment are known from allochthonous clasts recovered at Lonewolf Nunataks and include a variety of Cambrian, Proterozoic and Archean intermediate to silicic composition igneous and metamorphic rocks (Goodge and Fanning, 2010; Palmer, 2008; Palmer et al., 2012).

At Nimrod Glacier, the bedrock geology also varies along the valley. At the head of the Nimrod Glacier, outcrops at nunataks and in the Miller Range are Beacon/Ferrar Supergroup rocks and Proterozoic Nimrod Group rocks that are complexly intertwined with syntectonic Granite Harbor Intrusive Suite of Cambro-Ordovician age (Fig. 1). U-Pb zircon ages from Granite Harbor Intrusive Suite in the Miller Range are 493 ± 4 Ma to 545 ± 5 Ma (Goodge et al., 2012). The Nimrod Group rocks are igneous and high-grade metamorphic rocks that contain a complex record ranging from Archean magmatism (~3000 Ma) to the 1700 Ma Nimrod Orogeny; these rocks were deformed and overprinted in some cases during the Ross Orogeny (Goodge et al., 2001). As the Nimrod Glacier narrows, ice encounters rocks of the Neoproterozoic Beardmore Group siliciclastic rocks. The Beardmore Group includes sandstones and interbedded black shales of the Goldie Formation, a unit that is known to contain detrital zircon with U-Pb ages distributed between 1000-2000 Ma (Goodge et al., 2004). Downstream, the Nimrod Glacier crosses the Cambro-Ordovician Byrd Group and limited outcrops of the Granite Harbor Intrusive Suite (Fig. 1). The Byrd Group is diverse lithologically and includes the Shackleton Limestone as well as siliciclastic rocks ranging from conglomerates to

131 mudstones that record a transition from a passive margin to an active margin (forearc)
132 setting (Goodge et al., 2004; Myrow et al., 2002).

133 During the last glacial maximum (LGM) and numerous previous glacial periods,
134 grounded ice advanced onto the Ross Sea continental shelf depositing mud-rich diamicts
135 (Licht et al., 1999; McKay et al., 2009). Early workers analyzed sand provenance in
136 LGM tills and identified several lithologic provinces across the shelf (Anderson et al.,
137 1984). More detailed work on tills from both the Transantarctic Mountains and the Ross
138 Sea continental shelf identified a boundary in the central Ross Sea, indicating
139 convergence of East and West Antarctic ice sheet flow in this area during the LGM
140 (Farmer et al., 2006; Licht et al., 2005; Licht and Palmer, 2013). More detailed sampling
141 of Byrd Glacier tills (the same glacial sediments analyzed in study) used sand
142 petrography and detrital zircons to identify the origin of glacial debris and reconstruct
143 past ice flow paths of this major outlet into the Ross Sea continental shelf (Licht and
144 Palmer, 2013; Palmer et al., 2012). Reconstructions of ice flow from the Byrd Glacier
145 region to McMurdo Sound for time periods back to the Late Miocene, have utilized
146 geochemistry, sand and pebble lithology (Del Carlo et al., 2009; Hauptvogel and
147 Passchier, 2012; Monien et al., 2012; Panter et al., 2008; Talarico et al., 2012) and
148 detrital apatite (Zattin et al., 2012).

149 The composition and particle size of till in ice-cored moraines common in the
150 Transantarctic Mountains are useful for assessing the origin of the glacial debris.
151 Moraines along valley walls of large outlet glaciers are typically very thin (<10 cm), are
152 predominantly composed of local bedrock lithologies and have <15 % silt and clay
153 except where limestone outcrops (Licht and Palmer, 2013). In these locations, debris is
154 supplied englacially through debris-rich layers, experiences little comminution, and has
155 relatively short transport distances. Rock fall may also be a minor contributor. Nunatak
156 moraines are more complex and may either share characteristics of lateral moraines or
157 contain substantial subglacially-derived debris as indicated by abundance of erratics,
158 faceted/striated pebbles and >55% silt and clay (Palmer et al., 2012). The erratic
159 lithologies provide otherwise inaccessible information about the types of buried bedrock
160 (Goodge and Fanning, 2010; Palmer, 2008; Palmer et al., 2012), but little about the
161 specific location of origin. Generally, subglacial transport distances by continental ice

sheets are <100km, but can be much greater (Clark, 1987). The subglacial processes of abrasion and quarrying, along with variations in rock strength produce different particle size fractions and the eroded debris is incorporated into the base of the ice sheet in regions where waters freeze on (Hooke et al., 2013). All of these factors may impact interpretations in provenance studies.

3. Samples/Methods

Samples analyzed in this study are all ice-cored moraines from the Transantarctic Mountains (Fig. 1). The moraines are located along the lateral margins of the Byrd and Nimrod glaciers or occur adjacent to nunataks near the head of these glaciers. In all cases except Lonewolf 2 (LW2), the till drapes the ice and is <10 cm thick; at Lonewolf 2 till is >50 cm thick. The lateral sites are often along cliff faces and so may contain a component of rockfall, however, the abundance of silt and clay (~10-60%) plus visible debris rich bands in the ice indicate englacial debris input. Pebbles and cobbles in lateral moraines are rarely faceted or striated suggesting minimal subglacial input. All moraines are <1.7 km in length and the width of lateral moraines is <100 m.

Eighteen till samples were collected from moraines adjacent to five different groups of rocks (Table 1; Fig. 1). Nunatak sites on the inboard side of the Transantarctic Mountains were either Beacon/Ferrar Supergroup or Nimrod Group rocks. Lateral sites (outboard TAM) were adjacent to Granite Harbor Intrusives, Beardmore or Byrd Group rocks. Samples were collected after removing the top 1-2 cm to minimize the impacts of wind deflation and material was analyzed from single or multiple locations at each site. Both > 63μ and < 63μ size fractions were analyzed for Sr, Nd, and in some case Pb isotopes, along with a few cobbles from the moraine surface at Lonewolf Nunataks. Analytical methods for the Nd, Sr and Pb isotopic analyses are given in Table 1.

4. Results

In general, the till isotopic compositions vary systematically with downstream position in both the Byrd and Nimrod glacial drainages. Furthest upstream in the Byrd Glacier drainage, silt/clay (<63□) and sand (0.5 to 2.0 mm) fractions from both Lonewolf Nunatak tills samples (LW and LW2) collected adjacent to a nunatak of Beacon Supergroup rocks are characterized by low $\varepsilon_{Nd}(0)$ values (-19.5 to -20.3) (Fig. 2) and a

192 range of $^{87}Sr/^{86}Sr(0)$ 0.726 to 0.735 (Fig. 3). The Sr isotopic compositions correlate with
193 sediment Rb/Sr values and cluster around an ~560 Ma reference isochron. The sediments
194 also show a narrow range of Pb isotopic compositions that plot to the right of the
195 geochron on a $^{207}Pb/^{204}Pb$ vs. $^{206}Pb/^{204}Pb$ plot (Fig. 4) ($^{206}Pb/^{204}Pb$=18.25 to 18.54,
196 $^{207}Pb/^{204}Pb$=15.51 to 15.58). The two cobbles analyzed (LWE, LWI) have isotopic
197 compositions that are considerably different from those of the finer size fractions, having
198 $\varepsilon_{Nd}(0)$ ranging of -10 to -29 (respectively) and $^{87}Sr/^{86}Sr(0)$ from 0.7676 to 2.83 (Table 1).
199 Sample LWE also has significantly lower measured $^{206}Pb/^{204}Pb$ (16.6) and higher
200 $^{208}Pb/^{204}Pb$ (39.73) than the finer till samples.

201 Furthest upstream in the Nimrod Glacier drainage, <63μ till from Argo Glacier
202 and Milan Ridge have isotopic compositions similar to those from the Lonewolf Nunatak
203 with low $\varepsilon_{Nd}(0)$ (-15.5 to -18.5) (Fig. 2) and radiogenic Sr isotopic compositions that also
204 roughly align along a ~560 Ma reference isochron (Fig. 3). Lead isotopic compositions
205 are among the least radiogenic of any of the analyzed tills ($^{206}Pb/^{204}Pb$=18.03 to 18.16,
206 $^{207}Pb/^{204}Pb$=15.50 to 15.52, $^{208}Pb/^{204}Pb$=38.58 to 38.78; Fig. 4).

207 At sampling locations adjacent to nunataks of the Beacon and Ferrar Supergroup
208 rocks in both the Nimrod and Byrd Glacier catchments, the <63□ fraction of tills at All
209 Blacks, Bates Nunatak, Quest Cliffs, and Sanford Cliffs all have significantly higher
210 $\varepsilon_{Nd}(0)$ values, lower $^{87}Sr/^{86}Sr(0)$, higher uranogenic Pb isotopic ratios, but similar
211 $^{208}Pb/^{204}Pb$, compared to more inboard till samples (Figs. 2-4). The Sr isotopic
212 compositions generally cluster around an ~180 Ma reference isochron (Fig. 3). In
213 contrast, the <63 m tills from Brittania Ridge (Fig. 1) have lower $\varepsilon_{Nd}(0)$ (-10 to -15),
214 higher $^{87}Sr/^{86}Sr(0)$ (0.720 to 0.722) and more radiogenic Pb isotopic compositions (Figs.
215 2-4).

216 In the Nimrod Glacier catchment, two localities are adjacent to Beardmore Group
217 (Goldie Fm.), including the Kon Tiki in midstream of the main Nimrod Glacier and
218 Gargoyle Ridge along the Nimrod Glacier margin. The <63μ tills from both locations
219 have similar Nd isotopic compositions ($\varepsilon_{Nd}(0)$= -18.9 to -17.5) (Fig. 5), but the Kon Tiki
220 sample has higher $^{87}Sr/^{86}Sr(0)$ (0.736) (Fig. 6) and lower $^{207}Pb/^{204}Pb$ (15.6) than that from
221 Gargoyle Ridge (Fig. 7).

In the Byrd Glacier drainage, <63 □ tills from Mt. Tuatara are adjacent to exposure of the Shackleton Limestone of the Byrd Group. These samples have similar Nd isotopic compositions to upstream samples, but are characterized by low Sr and Nd contents (Table 1). These samples also have a wide range of $^{87}Sr/^{86}Sr$ (0) (0.716 to 0.782) that generally co-vary with $^{87}Rb/^{86}Sr$ (Fig. 6) along a ~560 Ma reference isochron. In the Nimrod Glacier drainage, tills from the Cambrian Bluff are found adjacent to the siliciclastic Starshot Formation of the Byrd Group (Myrow et al., 2002), and compared to the Mt. Tuatara tills have lower $\varepsilon_{Nd}(0)$ =-17.1 to -17.8, a more restricted range of $^{87}Sr/^{86}Sr(0)$=0.737 to 0.745, also roughly aligned along a ~560 Ma reference isochron (Fig. 6), and higher $^{208}Pb/^{204}Pb$ ratios (Fig. 7).

Finally, the furthest downstream tills in both the Byrd (Crazy Jim, Horney Bluff) and Nimrod (Campbell Hills) glacier drainages are found adjacent to, or in close proximity, to granitic rocks of the Granite Harbor Group. The <63μ tills at both locations have similar isotopic compositions that, compared to upstream tills, have higher $\varepsilon_{Nd}(0)$ (-12.3 to -13.6), but similar $^{87}Sr/^{86}Sr(0)$ =0.722 to 0.736, and Pb isotopic compositions (Figs. 5-7).

5. Discussion

Our principal observation is that the radiogenic isotopic composition of < 63μ tills vary regularly as a function of position in both the Byrd and Nimrod glacier drainages. The isotopic variations parallel changes in till petrography identified at some of the same sample locations (Licht and Palmer, 2013) as well as with the variations in bedrock composition present across the Transantarctic Mountains. The obvious conclusion is that the fine-grained tills at each sampled locality were derived from local bedrock lining the Byrd and Nimrod glaciers and represent either the products of direct abrasion of these rocks or further comminution of coarser grained sediments with which the fine-grained tills are associated.

A local bedrock source for the tills is particularly evident in the isotopic compositions of tills from inboard sample locations adjacent to the Beacon Supergroup (Sanford Cliffs, Quest Cliffs, All Blacks, Bates Nunatak, and Britannia Ridge). The bedrock is composed principally of Devonian to Early Jurassic sandstones (Beacon

252 Supergroup) intruded by dolerite sills and basaltic volcanic rocks of the mid-Jurassic
253 (~183 Ma) Ferrar Group (Barrett, 1991). The < 63μ size fraction till from most of these
254 localities have higher $\varepsilon_{Nd}(0)$ (> -10) and low $^{87}Sr/^{86}Sr$ (<0.720) compared to fine-grained
255 tills from other locations and these isotopic compositions overlap the values expected for
256 material eroded from the Ferrar Group igneous rocks (Figs. 2, 3). In fact, the Sr isotopic
257 compositions of fine-grained tills from Quest Cliffs, Sanford Cliffs, and Bates Nunatak,
258 align along the ~183Ma reference isochron defined by Ferrar Group igneous rocks (Fig
259 3). As a result Ferrar Group igneous rocks likely represent a primary component of the
260 fine-grained tills located adjacent to the Beacon Supergroup in both the Byrd and Nimrod
261 glacial drainages.

262 Basaltic igneous rocks, however, are not the sole contributor to these inboard
263 sediments. Till pebble fractions from the two locations where petrographic data are
264 available (Bates Nunatak and Britannia Ridge) are dominated by mafic lithologies but
265 also contain variable proportions of sandstone (Licht and Palmer, 2013), with the average
266 sandstone pebble abundances being considerably higher at the Britannia Ridge location
267 (~19%) compared to that at the Bates Nunataks (~7). No isotopic data are available from
268 the sand size sediments themselves, but average $\varepsilon_{Nd}(0)$ values for the Britannia Ridge
269 samples are also considerably lower (-12.5) than at the Bates Nunatak (-9.2) (Table 1)
270 The apparent correlation between decreasing $\varepsilon_{Nd}(0)$ in fine grained till and increasing
271 sandstone pebble abundances suggests that the < 63μ size fraction at both localities
272 represent further comminution of the sand sized tills and that sandstones from at least
273 portions of the Beacon Supergroup must have $\varepsilon_{Nd}(0)$ as low as -15. Such low $\varepsilon_{Nd}(0)$
274 values are typical of Precambrian continental crust and indicate the involvement of such
275 crust in the source of the sandstones, potentially cycled through inboard examples of the
276 Granite Harbor Intrusive Suite given the preponderance of detrital zircon in the age range
277 from 500 Ma to 650 Ma in the Beacon Supergroup sandstones as a whole (Elliot et al.,
278 2015). The Turret Nunatak samples, which are found in the Nimrod, rather than the Byrd
279 glacial drainage have identical isotopic characteristics to the low $\varepsilon_{Nd}(0)$ Brittania Ridge
280 sample and could represent erosion and comminution of similar starting materials.

281 Fine-grained tills from the Mt. Tuatara locality in the main Byrd glacial drainage
282 are another example of sediments derived from erosion of immediately adjacent bedrock,
283 in this case the Shackleton Limestone of the Byrd Group. The low Sr (5ppm to 37ppm)
284 and Nd (1.8ppm to 2.5ppm; Table 1) content of these samples likely reflects the
285 derivation of these sediments from erosion of local carbonate rocks, consistent with the
286 fact that 100% of the sand fraction at this locality is limestone and marble (Licht and
287 Palmer, 2013).

288 Outboard tills along the main trunks of both the Byrd and Nimrod glaciers
289 (Horney Bluff and Crazy Jim, and Campbell Hills, respectively) are all located adjacent
290 to early Cambrian Granite Harbor intrusive rocks, and contain pebble populations that
291 include both these intrusive rocks as well as abundant material derived from their
292 metaigneous wall rocks (Licht and Palmer, 2013). The Sr and Nd isotopic composition
293 of the < 63μ size fraction in these tills overlap those expected for detritus derived
294 exclusively from the Granite Harbor intrusive suite, and detrital zircons from the Crazy
295 Jim and Horney Bluff locality are dominantly ~530 Ma in age, also equivalent to the
296 local Granite Harbor granitic rocks (Licht and Palmer, 2013). These observations imply
297 that the sand and clay fractions from these tills are dominated by detritus from the
298 Granite Harbor igneous rocks. We conclude that the outboard tills can also be considered
299 as the products principally of the erosion of local bedrock.

300 The outboard tills samples also plot along early Cambrian Sr reference isochrons
301 (Fig. 6), including those samples from Gargoyle Ridge and Campbell Hills (Fig. 1).
302 Available data from bedrock in the Transantarctic Mountains demonstrate that whole
303 rock Rb-Sr isochrons defined by early Paleozoic and older rocks throughout Ross
304 Orogeny have been reset to this age (Goodge and Dallmeyer, 1992). That fact that our
305 outboard tills samples and bedrock align along Rb-Sr reference isochrons of similar age
306 again support the conclusion that the < 63μ sediments from all these localities are the
307 product of mechanical erosion of local bedrock.

308 The sources of fine-grained till at the most inboard till localities, adjacent to the
309 Lonewolf Nunataks (LW sites) in the Byrd glacial drainage and along the upstream
310 margins of the Miller Range in the Nimrod glacial drainage (MR and AG sites), may

311 present a situation distinct from their downstream counterparts given that several studies
312 of these tills have demonstrated that sand and pebble populations here include material
313 derived from the interior of East Antarctica (Goodge and Fanning, 2010; Palmer, 2008;
314 Palmer et al., 2012). Pebbles and sand from the LW locations have been the most
315 extensively studied, and these are clearly subglacial in origin and contain abundant
316 material, up to 35% at the LW sites, that are exotic to the local Beacon Supergroup and
317 Ferrar Group basement rocks (Palmer et al., 2012). The few isotopic analyses we have
318 from LW pebbles show a wide range of values including very low $\varepsilon_{Nd}(0)$ values that are
319 similar to Precambrian Nimrod Group basement (as exposed in Miller Range) and not to
320 the isotopic compositions expected for detritus derived from the Beacon Supergroup and
321 Ferrar Group, at least as estimated by the isotopic compositions we determined for our
322 Brittania Ridge, Bates Nunatak, and Turret Nunatak samples. So our data are consistent
323 with the possibility that sediments at some of the most inboard localities contain exotic
324 material derived from beneath the East Antarctic ice sheet. However, there are
325 insufficient isotopic analyses from pebbles and cobbles from the any of the inboard till
326 locations to assess whether the <63□ till fraction simply represents the comminution of
327 coarser grained material at these locations, as we concluded for most of our other till
328 samples, or instead have a provenance distinct from the coarser-grained till.

329 5.1. Sediment Transport

330 The goal of this study is to determine the sources of sediment currently
331 transported by glaciers in the central TAM, to assess the relative importance of erosion in
332 the TAM and the interior of East Antarctica in producing those sediments, and to
333 determine how the sources of present-day tills relate to the provenance of sediments
334 deposited during glacial maximum on the Ross Sea continental shelf. We address these
335 issues, and the implications our data have for assessing periods of grounding line retreat
336 for glaciers traversing the central TAM, in the following text.

337 5.1.1. Transantarctic Mountains

338 Till samples from the Nimrod and Byrd glaciers demonstrate that tills along the
339 margins of the main trunk of both glaciers contain sediment exclusively derived from
340 local bedrock. Although material is delivered by englacial debris bands, transport

distances must be very limited and lateral moraines positions may be related to locations where bedrock is not far below the ice surface. In contrast, tills from locations adjacent to the mid-stream Lonewolf Nunataks sample subglacial tills entering the TAM and include exotic material likely derived from more sources further into the interior of the East Antarctic ice sheet, albeit not likely from more than 100 km further inboard (Licht and Palmer, 2013). An important question is whether such exotic material remains an important component of the glacier's debris load as the ice flows through narrow outlet glaciers across the TAM.

KonTiki Nunatak is similar to the Lonewolf Nunatak in that it is a small outcrop that occurs in the middle of the Nimrod Glacier. The <63μ fraction of till from this location has Pb, Sr and Nd isotopic compositions essentially identical to those from the Lonewolf Nunatak moraines and suggest that the sources of subglacial tills at this position downstream in the Nimrod Glacier are equivalent to those sampled further inboard. One option is that the KonTiki Nunatak tills represents sedimentary material derived from the interior of East Antarctica transported through the TAM by the Nimod Glacier and that such sediments are the dominant component of subglacial tills even halfway through their traverse of the mountain range. However, we note the KonTiki Nunatak, and adjacent portions of the Nimrod Glacier valley, are composed of the Neoproterozoic Beardmore Group, specifically the "inboard" Beardmore Group of Goodge et al (2002). This sedimentary unit consists of siliciclastic sedimentary rock, carbonate and minor mafic volcanic rocks in two mappable units (the Cobham and Goldie Formations). Detrital zircons from these bedrock units are 1 Ga or older, with no evidence of any detrital material contemporaneous with the Ross Orogeny (Goodge et al., 2002; Goodge et al., 2004). Previous workers have concluded that the inboard Beardmore Group is an authochthonous, passive margin sedimentary succession derived from the erosion of the adjacent Archean to Proterozoic age East Antarctic craton, the same general material from which the Lonewolf Nunatak and Miller Range tills were likely derived. It is possible that the isotopic compositions of Beardmore Group in the vicinity of Gargoyle Ridge and Kon Tiki Nunatak are similar to those of the "input" sediment and as a result, the isotopic compositions of till in this region are the result of the fact that these sediments were derived from comminution of these low $\varepsilon_{Nd}(0)$ local

372 bedrocks, and do not represent an emerging low $\varepsilon_{Nd}(0)$ subglacial till. Isotopic data from
373 the local bedrock are not available to test this assertion. Isotopic data from the "Goldie"
374 Formation that are available are from the "outboard" Beardmore group in the central
375 TAM (Borg et al., 1990), which are now considered to be Lower Cambrian in age and
376 correlative with the Byrd Group (Myrow et al., 2002). The Nd isotopic composition of
377 these rocks are significantly higher than those of the Kon-Tiki and GR tills (Fig. 5), but
378 this could be because these rocks contain significant amounts of younger, syn-Ross
379 Orogeny volcaniclastic and other siliciclastic sediments, and were not exclusively derived
380 from low $\varepsilon_{Nd}(0)$ Archean to Proterozoic age basement.

381 *5.1.2. Ross Sea*

382 Previous studies demonstrated that $\varepsilon_{Nd}(0)$ values increase, $^{87}Sr/^{86}Sr$ (0) decrease
383 and Pb isotopic compositions become more radiogenic for the <63μ size fraction in LGM
384 tills deposited from the central to western Ross Sea (Farmer et al., 2006). Based on a
385 comparison to the isotopic compositions of a limited set of till samples from the
386 Beardmore and Darwin-Hatherton Glaciers in the TAM, Farmer et al. (2006) concluded
387 that fine-grained LGM tills in the western half of the Ross Sea were deposited during
388 expansion of the East Antarctic ice sheet, and that the tills incorporated an increasing
389 proportion, from east to west, of detritus eroded from Late Cenozoic volcanic rocks
390 bordering and/or underlying the western Ross Sea. These conclusions are strengthened
391 by the addition of our new onshore till data from the Nimrod and Byrd glaciers. The Pb,
392 Sr, and Nd isotopic compositions of the <63μ LGM tills in the central Ross Sea all
393 overlap the values expected for mechanical mixtures of glacial detritus similar
394 isotopically to the fine-grained tills analyzed from these two glacial drainages (Fig. 8-10).
395 The few isotopic analyses available from the Darwin-Hatherton glaciers reported in
396 Farmer et al. (2006) also plot within the range of isotopic compositions defined by the
397 Byrd and Nimrod glaciers, all of which provide strong evidence that the fine-grained
398 central Ross Sea LGM tills are dominated by detritus delivered by glaciers traversing the
399 central TAM.

400 In contrast, none of the onshore tills analyzed from the Byrd and Nimrod
401 glaciers, including tills derived from the Ferrar dolerites, have sufficiently high $\varepsilon_{Nd}(0)$ or

low $^{87}Sr/^{86}Sr(0)$ to account for the entire range of isotopic compositions observed in tills from the western Ross Sea (Fig. 8-10). To account for the highest $\varepsilon_{Nd}(0)$, and lowest $^{87}Sr/^{86}Sr(0)$ observed for the <63μ tills in the western Ross Sea, Farmer et al. (2006) suggested that these sediments and onshore tills bordering McMurdo Sound (e.g. Pyramid Fuel Cache sample from Farmer et al., 2006; Figs. 8-10) contain a contribution from Cenozoic McMurdo volcanic suite rocks. The latter are exposed onshore adjacent to the western Ross Sea and have higher $\varepsilon_{Nd}(0)$ (0 to +5), lower $^{87}Sr/^{86}Sr(0)$ (0.7030 to 0.7050) than the Ferrar dolerites as well as a wide range of Pb isotopic compositions (Martin et al., 2013). Our new data from the Byrd and Nimrod glacial tills are generally consistent with this interpretation, as is the observation that the proportions of basaltic sand and rock fragments in LGM tills increase from the central to western Ross Sea (Giorgetti et al., 2009; Licht et al., 2005). All of the above observations suggest that the McMurdo volcanic rocks experienced active erosion by ice expanding through the TAM during the Last Glacial Maximum.

Because the isotopic compositions of modern tills associated with both the Byrd and Nimrod glaciers vary as a function of position along the TAM, and because detritus eroded from such lithologies as the Ferrar dolerites and the Granite Harbor intrusive rocks have distinctive isotopic compositions, it may be possible to assess whether specific locations and or rocks types within the TAM or further inboard into East Antarctica were contributing disproportionately to LGM sediment deposited in Ross Sea. Defining where sediment production was greatest along ice flow trajectories in the TAM could be useful in determining ice conditions (basal temperature, velocity, etc.) in this region during the Last Glacial Maximum (Golledge et al., 2013; Jamieson et al., 2010).

We found that the Nd, Sr and Pb isotopic compositions of the central Ross Sea fine-grained tills are difficult to attribute to the erosion of specific TAM lithologies. For example, the Lonewolf Nunatak tills are isotopically distinctive but none of the < 63μ tills in the central Ross have sufficiently low $\varepsilon_{Nd}(0)$ values, or high $^{87}Sr/^{86}Sr(0)$, to be derived predominately from such detritus. Clearly sediments derived from the interior of East Antarctica or from the most inboard portions of the Byrd Glacier catchment do not represent the dominant component of < 63μ deposited during the LGM in the Ross Sea.

Similarly, no central Ross Sea tills have sufficiently high $^{208}Pb/^{204}Pb$ or $^{87}Sr/^{86}Sr$ ratios (Fig. 8-10) to be the products predominately of the erosion of "outboard" Granite Harbor igneous rocks. The relatively low $^{87}Sr/^{86}Sr$ and $^{208}Pb/^{204}Pb$ ratios of the central Ross Sea tills, however, do suggest that Ferrar dolerites exposed in inboard positions in the central TAM must have contributed to this detritus. Our conclusion, then, is that fine-grained LGM tills in the central Ross Sea are best interpreted as mechanical mixtures of detritus eroded from rocks encountered by ice flowing through the TAM, including inputs from bedrock inland of the narrowest part of the glacial valleys. If single lithologies dominated the glacial detritus generated during the LGM, it is not evident from the available isotopic data.

Sediment production associated with ice flow through TAM outlets, such as the Byrd Glacier, is considered to be greatest where ice velocity is at a maximum and subglacial water is produced (Fig. 11) (Jamieson et al., 2010; Golledge 2013), Since the likelihood of basal melt increases as ice velocity increases, one might expect that subglacial debris entrained inland of the narrow glacial valleys would melt out and be absent downstream of the outlet mouths. However, our data from fine-grained tills in the central Ross Sea suggest that during the LGM, sediment was derived from both the highest velocity regions of the outlet glacier, as well as upstream bedrock sources where ice had not reached its maximum velocity. Therefore, we infer that debris entrained from upstream sources is transported englacially or that subglacial deformation is an efficient transport mechanism over distances of hundreds of kilometers in this setting. Evidence in support of englacial transport comes from a numerical model of Byrd Glacier showing that basal ice trajectories are upward in the catchment area upstream of the main trunk (Golledge et al., 2013). This can explain both the occurrence of the moraine at Lonewolf Nunatak and also the long travel distances as the entrained sediment follows an upward trajectory, preventing basal melt out.

Detrital zircon U-Pb ages from sand size fraction of central Ross Sea LGM tills are also consistent with multiple sources for this coarser detritus. Specifically, the dominant U-Pb age population in central Ross Sea tills has a broad range of zircon ages 520- 600 Ma that were most likely derived from granitic rocks formed during the Neoproterozoic to Cambrian Ross-Pan African Orogeny. Zircons from tills adjacent to

463 the Cambrian Granite Harbor intrusive suite rocks along Byrd Glacier range from 520 Ma
464 to 540 Ma, and therefore these granitic rocks contributed to, but were not the sole source
465 of, Neoproterozoic to Cambrian zircons in Ross Sea tills. The abundant older zircons
466 (560-600 Ma) are interpreted to have been derived from Beacon Supergroup or older,
467 unexposed Granite Harbor suite intrusive rocks upstream of the narrow glacial valleys of
468 the Byrd and Nimrod glaciers (Elliot et al., 2015; Elliot and Fleming, 2008; Elsner et al.,
469 2013; Licht et al., 2014; Licht and Palmer, 2013). As a result, both the detrital zircons
470 and radiogenic isotopic data can be interpreted as providing evidence that sediments
471 deposited in the central Ross Sea during the LGM represent erosion along the narrow
472 valleys of the outlet glaciers, as well as areas further inland.

473 Our data illustrate that neither the U-Pb detrital zircon ages or the radiogenic
474 isotope data unambiguously define the exact sources of the sediments that contributed to
475 the Ross Sea till. Nevertheless, the two approaches have their own specific advantages in
476 in determining the till provenance. The radiogenic isotopic data, for example, reveal the
477 importance of zircon-poor lithologies such as the Ferrar dolerites and the McMurdo
478 Group volcanic rocks in the sources of the fine-grained Ross Sea sediment. The detrital
479 zircon data, in turn, reveal the potential importance of the erosion of the Beacon
480 Supergroup in providing coarse detritus Ross Sea during the LGM, a conclusion that
481 could not readily be drawn from the sediment Nd, Sr or Pb isotopic compositions.

482 5.2. *Potential for Ice Extent Determinations in central Transantarctic Mountains*

483 Our data illustrate that LGM tills in the central Ross Sea likely contain detritus
484 eroded by outlet glaciers along their entire traverse through the central TAM. This
485 observation suggests that other expansions of ice extent through TAM in the past would
486 produce glaciomarine deposits with a similarly complex provenance. Such ice advances
487 also clearly involve the erosion by grounded ice of Late Cenozoic McMurdo Volcanic
488 Suite rocks found along the eastern flank of the TAM adjacent to the western Ross Sea
489 (Monien et al., 2012). Our data also illustrate, however, that ice sheet grounding line
490 retreat inland of the narrow valleys cutting the TAM could produce changes in the
491 provenance of glacial sediments recognizable both through detrital zircon U-Pb ages in
492 coarser detritus and through radiogenic isotope analyses of finer grained material. For

example, if glacial erosion were isolated to the inboard portions of the TAM, then detrital zircons related to the Ross Orogeny might be restricted to older (560 Ma to 600 Ma) sources and the proportion of sediment with low $\varepsilon_{Nd}(0)$ values (<-5) should increase, as the amount of sediment derived from Precambrian basement rocks beneath the EAIS and/or from the Beacon Formation increases.

6. Conclusions

Our data provide clear evidence that tills in lateral moraines along the margins of the Nimrod and Byrd glacial drainages today are predominantly derived from erosion of local bedrock within the Transantarctic Mountains, although some nunatak moraines contain material transported from more distal locations beneath East Antarctic ice sheet. For those lateral moraines for which data from different till size fractions are available, the silt/clay, sand and pebble sized materials share the same provenance, indicating that fine grained sediment represent the comminution of coarser grained till. We also demonstrate that the Nd, Sr and Pb isotopic values from <63μ tills in the central-western Ross Sea are dominated by detritus generated within and adjacent to the TAM, presumably along the same troughs that confine major outlet glaciers today, a conclusion consistent with previously published detrital zircon provenance data from central Ross Sea tills (Licht and Palmer, 2013). The results of this study also reveal that it may be able to track past ice grounding line retreats through the TAM via glaciomarine sediments, given the observations that regular and identifiable variations U-Pb detrital zircon ages and radiogenic isotope compositions exist in till produced across the strike of the mountain range today.

7. Acknowledgements

This material is based upon work supported by the National Science Foundation under Grant No. OPP-0440177 to the University of Colorado and OPP-0440885 to IUPUI. We are grateful to field team members D. Brecke, A. Barth, P. Braddock, and J. Goodge, as well as Crazy Jim Haffey of Ken Borek Air, Ltd. and Raytheon Polar Services. Comments by the journal reviewers resulted in substantial improvements to the manuscript.

8. Figure Captions

Fig. 1- Till sample locations shown on Radarsat basemap. Schematic bedrock geology after Gridley and Laird (1969) and Myrow et al. (2002). Inset map shows general location of Ross Sea cores for which LGM glacial sediment isotopic analyses are available (Farmer et al., 2006). BN = Bates Nunatak, BR = Brittania Ridge, CJ = Crazy Jim, HB = Horney Bluff, MT = Mt. Tuatara, LW/LW2 = Lonewolf Nunataks, AB = All Blacks Nunatak, QC = Quest Cliffs, TN = Turret Nunatak, GR = Gargoyle Ridge, CB = Cambrian Bluff, CH = Campbell Hills, KT = KonTiki Nunatak, MR = Milan Ridge, AG = Argo Glacier, SC = Sanford Cliffs.

Fig. 2- Measured $\varepsilon_{Nd}(0)$ vs. $^{147}Sm/^{144}Nd$ for tills from western (inboard) portions of TAM. Ferrar basalt/dolerite data from Antonini et al. (1999) and Elliot et al. (1999). Miller Range Granite Suite intrusive rock and basement data from Borg et al., 1990. The 1.4 Ga granite clast (TNQ) is from a moraine in the upper Nimrod Glacier; data reported in Goodge et al. (2008).

Fig. 3- Measured $^{87}Sr/^{86}Sr$ vs. $^{87}Rb/^{86}Sr$ for tills from western (inboard) portions of TAM. Ferrar basalt and dolerite data from Antonini et al. (1999) and Elliot et al. (1999). Data for Precambrian basement and Granite Harbor Intrusive Suite rocks in Miller Range from Borg et al. (1990).

Fig. 4- Measured Pb isotopic data for tills from western (inboard) of TAM. Shaded areas are central Ross Sea are data from LGM tills from cores in this region from Farmer et al. (2006). Analysis from surface till from Pyramid Fuel Cache also from Farmer et al. (2006). Range of Ferrar basalt isotopic data from Antonini et al. (1999).

Fig. 5- Measured ε_{Nd} vs. $^{147}Sm/^{144}Nd$ for tills from eastern (outboard) portions of TAM. Data ranges for Goldie Formation and for Granite Harbor Intrusive suite samples from Borg et al., 1990. Field for Lonewolf Nunataks from Fig. 2.

Fig. 6- Measured $^{87}Sr/^{86}Sr$ vs. $^{87}Rb/^{86}Sr$ for tills from eastern (outboard) portions of TAM. References for data from Ferrar dolerites, Goldie Formation and Granite Harbor Intrusive Suite rocks as in Fig. 2.

551 **Fig. 7**- Measured Pb isotopic data for tills from eastern (outboard) of TAM. Data
552 references as in Fig. 4.

553 **Fig. 8**- Measured ε_{Nd} vs. 1/Nd for < 63 μ size fractions from LGM tills in central and
554 western Ross Sea cores (shaded area; Farmer et al., 2006) relative to average Byrd and
555 Nimrod till isotopic compositions. Hatched curves are conventional two-component
556 mixing lines (Albarede, 1995) between average < 63 μ size fractions from tills in Byrd
557 and Nimrod glacial drainages adjacent to "outboard" Granite Harbor Intrusive Suite
558 rocks, Ferrar dolerite, and Beacon Supergroup (Lonewolf Nunataks). Hatches show 0.1
559 increments in mass fraction of two components in a given mixture. Range of ε_{Nd} (0)
560 values for McMurdo Volcanic Group rocks are from Mount Morning in Victoria Land
561 (Martin et al., 2013). Data for <63μ from Darwin and Beardmore Glaciers from Farmer et
562 al. (2006).

563 **Fig. 9**- Measured $^{87}Sr/^{86}Sr$ vs. 1/Sr for < 63μ size fractions from LGM tills in central and
564 western Ross Sea cores (Farmer et al., 2006). Two-component mixing lines calculated as
565 in Fig. 8. References for other data shown given in Fig. 8 caption.

566 **Fig. 10**- $^{208}Pb/^{204}Pb$ vs. $^{206}Pb/^{204}Pb$ for < 63μ size fractions from LGM tills in central and
567 western Ross Sea cores (Farmer et al., 2006). Two-component mixing lines calculated as
568 in Fig. 8. References for other data shown given in caption for Fig. 8.

569 **Fig 11-** Maps of ice flow paths, velocity and erosion potential for Byrd and Nimrod
570 glacier. Map orientations as in Figure 1. a) Modern ice flow paths and velocity indicated
571 by shading. Orange (light grey) is lowest and purple (dark grey) is highest. The highest
572 velocities occur where flow is funneled through outlet glacier valleys. High velocity
573 should enhance erosion. For Byrd Glacier, km-scale spatial variability in bed conditions
574 (van der Veen et al., 2014) cause more complex patterns of erosion rates than suggested
575 by these large-scale models. B=Byrd Glacier and N=Nimrod Glacier catchments.
576 b) Modeled basal erosion potential for the LGM; darker gray reflects higher potential
577 (~10 mm/yr) (modified from Golledge et al., 2013). The erosion potential is a function of
578 basal shear stress, velocity and sediment cover on the bed.
579 c) Modeled ice flow paths for the LGM (modified from Golledge et al., 2013) over
580 modern grounded ice extent, dark gray shaded area. Blue shaded area highlights Nimrod

581 Glacier catchment and light gray area highlights the Byrd Glacier catchment. Ross Sea
582 core locations shown by yellow triangles. Green ovals highlight onshore sample areas
583 and regions of ice flow with the highest velocity.

584

585 **9. References**

586 Albarède, F., 1995, Introduction to Geochemical Modeling, Cambridge University Press,
587 Cambridge, 543 pp.

588 Alley, R. B., Cuffey, K. M., Evenson, E. B., Strasser, J. C., Lawson, D. E., and Larson,
589 G. J., 1997, How glaciers entrain and transport basal sediment: Physical
590 constraints: Quaternary Science Reviews, v. 16, no. 9, p. 1017-1038.

591 Anderson, J. B., Brake, C. F., and Myers, N. C., 1984, Sedimentation on the Ross Sea
592 Continental-Shelf, Antarctica: Marine Geology, v. 57, no. 1-4, p. 295-333.

593 Anderson, J. M., 1979, The geology of the Taylor Group, Beacon Supergroup, Byrd
594 Glacier area, Antarctica: Antarctic Record, v. 2, p. 6-11.

595 Antonini, P., Piccirillo, E. M., Petrini, R., Civetta, L., D'Antonio, M., and Orsi, G.,
596 1999, Enriched mantle–Dupal signature in the genesis of the Jurassic Ferrar
597 tholeiites from Prince Albert Mountains (Victoria Land, Antarctica):
598 Contributions to Mineralogy and Petrology, v. 136, no. 1, p. 1-19.

599 Austermann, J., Pollard, D., Mitrovica, J. X., Moucha, R., Forte, A. M., DeConto, R. M.,
600 Rowley, D. B., and Raymo, M. E., 2015, The impact of dynamic topography
601 change on Antarctic ice sheet stability during the mid-Pliocene warm period:
602 Geology, v. 43, no. 10, p. 927-930.

603 Barrett, P. J., 1991, Antarctica and Global Climatic-Change - a Geological Perspective:
604 Antarctica and Global Climatic Change, p. 35-50.

605 Borg, S. G., DePaolo, D. J., and Smith, B. M., 1990, Isotopic Structure and Tectonics of
606 the Central Transantarctic Mountains: Journal of Geophysical Research-Solid
607 Earth and Planets, v. 95, no. B5, p. 6647-6667.

608 Clark, P. U., 1987, Subglacial sediment dispersal and till composition: The Journal of
609 Geology, p. 527-541.

610 Cook, C. P., van de Flierdt, T., Williams, T., Hemming, S. R., Iwai, M., Kobayashi, M.,
611 Jimenez-Espejo, F. J., Escutia, C., Gonzalez, J. J., Khim, B. K., McKay, R. M.,
612 Passchier, S., Bohaty, S. M., Riesselman, C. R., Tauxe, L., Sugisaki, S., Galindo,
613 A. L., Patterson, M. O., Sangiorgi, F., Pierce, E. L., Brinkhuis, H., and Scientists,
614 I. E., 2013, Dynamic behaviour of the East Antarctic ice sheet during Pliocene
615 warmth: Nature Geoscience, v. 6, no. 9, p. 765-769.

616 Creyts, T. T., Ferraccioli, F., Bell, R. E., Wolovick, M., Corr, H., Rose, K. C., Frearson,
617 N., Damaske, D., Jordan, T., Braaten, D., and Finn, C., 2014, Freezing of ridges
618 and water networks preserves the Gamburtsev Subglacial Mountains for millions
619 of years: Geophysical Research Letters, v. 41, no. 22, p. 8114-8122.

620 Del Carlo, P., Panter, K. S., Bassett, K., Bracciali, L., Di Vincenzo, G., and Rocchi, S.,
621 2009, The upper lithostratigraphic unit of ANDRILL AND-2A core (Southern
622 McMurdo Sound, Antarctica): Local Pleistocene volcanic sources,
623 paleoenvironmental implications and subsidence in the southern Victoria Land
624 Basin: Global and Planetary Change, v. 69, no. 3, p. 142-161.

625 Dolan, A. M. e. a., 2011, Sensitivity of Pliocene ice sheets to orbital forcing: Paleogeogr.
626 Paleoclimatol. Paleoecol., v. 309, p. 98–110.

627 Elliot, D. H., 2013, The geological and tectonic evolution of the Transantarctic
628 Mountains: a review: Geological Society, London, Special Publications, v. 381,
629 no. 1, p. 7-35.

630 Elliot, D. H., Fanning, C. M., and Hulett, S. R. W., 2015, Age provinces in the Antarctic
631 craton: Evidence from detrital zircons in Permian strata from the Beardmore
632 Glacier region, Antarctica: Gondwana Research, v. 28, no. 1, p. 152-164.

633 Elliot, D. H., and Fleming, T. H., 2008, Physical volcanology and geological
634 relationships of the Jurassic Ferrar Large Igneous Province, Antarctica: Journal of
635 Volcanology and Geothermal Research, v. 172, no. 1-2, p. 20-37.

636 Elliot, D. H., Fleming, T. H., Kyle, P. R., and Foland, K. A., 1999, Long-distance
637 transport of magmas in the Jurassic Ferrar large igneous province, Antarctica:
638 Earth and Planetary Science Letters, v. 167, no. 1, p. 89-104.

639 Elsner, M., Schoner, R., Gerdes, A., and Gaupp, R., 2013, Reconstruction of the early
640 Mesozoic plate margin of Gondwana by U-Pb ages of detrital zircons from
641 northern Victoria Land, Antarctica: Antarctica and Supercontinent Evolution, v.
642 383, p. 211-232.

643 Farmer, G. L., Licht, K., Swope, R. J., and Andrews, J., 2006, Isotopic constraints on the
644 provenance of fine-grained sediment in LGM tills from the Ross Embayment,
645 Antarctica: Earth and Planetary Science Letters, v. 249, no. 1-2, p. 90-107.

646 Foley, D. J., Stump, E., van Soest, M., Whipple, K. X., and Hodges, K. V., 2013,
647 Differential Movement across Byrd Glacier, Antarctica, as indicated by Apatite
648 (U-Th)/He thermochronology and geomorphological analysis: Geological
649 Society, London, Special Publications, v. 381, no. 1, p. 37-43.

650 Giorgetti, G., Talarico, F., Sandroni, S., and Zeoli, A., 2009, Provenance of Pleistocene
651 sediments in the ANDRILL AND-1B drillcore: Clay and heavy mineral data:
652 Global and Planetary Change, v. 69, no. 3, p. 94-102.

653 Golledge, N. R., Levy, R. H., McKay, R. M., Fogwill, C. J., White, D. A., Graham, A. G.
654 C., Smith, J. A., Hillenbrand, C.-D., Licht, K. J., Denton, G. H., Ackert, J., Robert
655 P, Maas, S. M., and Hall, B. L., 2013, Glaciology and geological signature of the

Last Glacial Maximum Antarctic ice sheet: Quaternary Science Reviews, v. 78, p. 225-247.

Goodge, J. W., and Dallmeyer, R. D., 1992, $^{40}Ar/^{39}Ar$ Mineral Age Constraints on the Paleozoic Tectonothermal Evolution of High-Grade Basement Rocks within the Ross Orogen, Central Transantarctic Mountains: Journal of Geology, v. 100, p. 91-106.

Goodge, J. W., and Fanning, C. M., 2010, Composition and age of the East Antarctic Shield in eastern Wilkes Land determined by proxy from Oligocene-Pleistocene glaciomarine sediment and Beacon Supergroup sandstones, Antarctica: Geological Society Of America Bulletin, v. 122, no. 7-8, p. 1135-1159.

Goodge, J. W., Fanning, C. M., and Bennett, C. V., 2001, U-Pb evidence of similar to 1.7 Ga crustal tectonism during the Nimrod Orogeny in the Transantarctic Mountains, Antarctica: implications for Proterozoic plate reconstructions: Precambrian Research, v. 112, no. 3-4, p. 261-288.

Goodge, J. W., Fanning, C. M., Norman, M. D., and Bennett, V. C., 2012, Temporal, Isotopic and Spatial Relations of Early Paleozoic Gondwana-Margin Arc Magmatism, Central Transantarctic Mountains, Antarctica: Journal of Petrology, v. 53, no. 10, p. 2027-2065.

Goodge, J. W., Myrow, P., Williams, I. S., and Bowring, S. A., 2002, Age and provenance of the Beardmore Group, Antarctica: constraints on Rodinia supercontinent breakup: The Journal of Geology, v. 110, no. 4, p. 393-406.

Goodge, J. W., Vervoort, J. D., Fanning, C. M., Brecke, D. M., Farmer, G. L., Williams, I. S., Myrow, P. M., and DePaolo, D. J., 2008, A positive test of east Antarctica-Laurentia juxtaposition within the Rodinia supercontinent: Science, v. 321, no. 5886, p. 235-240.

Goodge, J. W., Williams, I. S., and Myrow, P., 2004, Provenance of Neoproterozoic and lower Paleozoic siliciclastic rocks of the central Ross orogen, Antarctica: Detrital record of rift-, passive-, and active-margin sedimentation: Geological Society Of America Bulletin, v. 116, no. 9, p. 1253.

Grindley, G. W., and Laird, M. G., 1969, , in Bushnell, V.C., and Craddock, C., eds., Geologic Map of Antarctica: , folio 12, sheet 15, scale 1:1,000,000., 1969, Geology of the Shackleton Coast, Antarctica,, scale 1:1,000,000.

Hauptvogel, D. W., and Passchier, S., 2012, Early-Middle Miocene (17-14 Ma) Antarctic ice dynamics reconstructed from the heavy mineral provenance in the AND-2A drill core, Ross Sea, Antarctica: Global and Planetary Change, v. 82-83, p. 38-50.

691 Hooke, R. L., Cummings, D. I., Lesemann, J. E., and Sharpe, D. R., 2013, Genesis of
692 dispersal plumes in till: Canadian Journal of Earth Sciences, v. 50, no. 8, p. 847-
693 855.

694 Humbert, A., Greve, R., and Hutter, K., 2005, Parameter sensitivity studies for the ice
695 flow of the Ross Ice Shelf, Antarctica: Journal of Geophysical Research, v. 110,
696 no. F4, p. n/a-n/a.

697 Jamieson, S. S. R., Sugden, D. E., and Hulton, N. R. J., 2010, The evolution of the
698 subglacial landscape of Antarctica: Earth and Planetary Science Letters, v. 293,
699 no. 1-2, p. 1-27.

700 Licht, K. J., Dunbar, N. W., Andrews, J. T., and Jennings, A. E., 1999, Distinguishing
701 subglacial till and glacial marine diamictons in the western Ross Sea, Antarctica:
702 Implications for a last glacial maximum grounding line: Geological Society of
703 America Bulletin, v. 111, no. 1, p. 91-103.

704 Licht, K. J., Hennessy, A. J., and Welke, B. M., 2014, The U-Pb detrital zircon signature
705 of West Antarctic ice stream tills in the Ross embayment, with implications for
706 Last Glacial Maximum ice flow reconstructions: Antarctic Science, v. 26, no. 6, p.
707 687-697.

708 Licht, K. J., Lederer, J. R., and Swope, R. J., 2005, Provenance of LGM glacial till (sand
709 fraction) across the Ross embayment, Antarctica: Quaternary Science Reviews, v.
710 24, no. 12-13, p. 1499-1520.

711 Licht, K. J., and Palmer, E. F., 2013, Erosion and transport by Byrd Glacier, Antarctica
712 during the Last Glacial Maximum: Quaternary Science Reviews, v. 62, p. 32-48.

713 Martin, A. P., Cooper, A. F., and Price, R. C., 2013, Petrogenesis of Cenozoic, alkalic
714 volcanic lineages at Mount Morning, West Antarctica and their entrained
715 lithospheric mantle xenoliths: Lithospheric versus asthenospheric mantle sources:
716 Geochimica et Cosmochimica Acta, v. 122, no. C, p. 127-152.

717 McKay, R., Browne, G., Carter, L., Cowan, E., Dunbar, G., Krissek, L., Naish, T.,
718 Powell, R., Reed, J., Talarico, F., and Wilch, T., 2009, The stratigraphic signature
719 of the late Cenozoic Antarctic Ice Sheets in the Ross Embayment: Geological
720 Society Of America Bulletin, v. 121, no. 11-12, p. 1537-1561.

721 Monien, D., Kuhn, G., von Eynatten, H., and Talarico, F. M., 2012, Geochemical
722 provenance analysis of fine-grained sediment revealing Late Miocene to recent
723 Paleo-Environmental changes in the Western Ross Sea, Antarctica: Global and
724 Planetary Change, v. 96-97, p. 41-58.

725 Myrow, P. M., Pope, M. C., Goodge, J. W., Fischer, W., and Palmer, A. R., 2002,
726 Depositional history of pre-Devonian strata and timing of Ross orogenic

727 tectonism in the central Transantarctic Mountains, Antarctica: Geological Society
728 Of America Bulletin, v. 114, no. 9, p. 1070-1088.

729 Palmer, E. F., 2008, Rock, till, and ice: A provenance study of the Byrd Glacier and
730 central and western Ross Sea, AntarcticaMSc.]: Indianapolis, Indiana University,
731 191 p.

732 Palmer, E. F., Licht, K. J., Swope, R. J., and Hemming, S. R., 2012, Nunatak moraines as
733 a repository of what lies beneath the East Antarctic ice sheet, Volume 487,
734 Geological Society of America, p. 97-104.

735 Panter, K. S., Talarico, F. M., Bassett, K., DelCarlo, P., Feild, B., Frank, T., Hoffmann,
736 S., Kuhn, G., Reichelt, L., Sandroni, S., Taviani, M., Bracciali, L., Cornamusini,
737 G., vonEynatten, H., Rocchi, S., and Team, A.-S. S., 2008, Petrologic and
738 geochemical composition of the AND-2A, ANDRILL Southern McMurdo Sound
739 Project, Antarctica: Terra Antarctica, v. 15, p. 147-192.

740 Stump, E., Gootee, B., and Talarico, F., 2006, Tectonic model for development of the
741 Byrd Glacier discontinuity and surrounding regions of the Transantarctic
742 Mountains during the neoproterozoic early paleozoic: Antarctica: Contributions to
743 Global Earth Sciences, p. 181-190.

744 Stump, E., Gootee, B. F., Talarico, F., Van Schmus, W. R., Brand, P. K., Foland, K. A.,
745 and Fanning, C. M., 2004, Correlation of Byrd and Selborne Groups, with
746 implications for the Byrd Glacier discontinuity, central Transantarctic Mountains,
747 Antarctica: New Zealand Journal of Geology and Geophysics, v. 47, no. 2, p. 157-
748 171.

749 Sugden, D. E., 1996, The East Antarctic Ice Sheet: Unstable ice or unstable ideas?:
750 Transactions of the Institute of British Geographers, v. 21, no. 3, p. 443-454.

751 Talarico, F. M., McKay, R. M., Powell, R. D., Sandroni, S., and Naish, T., 2012, Late
752 Cenozoic oscillations of Antarctic ice sheets revealed by provenance of basement
753 clasts and grain detrital modes in ANDRILL core AND-1B: Global and Planetary
754 Change, v. 96-97, p. 23-40.

755 Van der Veen, C. J., Stearns, L. A., Johnson, J. and Csatho, B., 2014, Flow dynamics of
756 Byrd Glacier, East Antarctica, J. of Glaciology, v. 60, n. 224, p. 1053-1064.

757 Winnick, M. J., and Caves, J. K., 2015, Oxygen isotope mass-balance constraints on
758 Pliocene sea level and East Antarctic Ice Sheet stability: Geology, v. 43, no. 10, p.
759 879-882.

760 Yokoyama, Y., Anderson, J. B., Yamane, M., Simkins, L. M., Miyairi, Y., Yamazaki, T.,
761 Koizumi, M., Suga, H., Kusahara, K., Prothro, L., Hasumi, H., Southon, J. R., and

762 Ohkouchi, N., 2016, Widespread collapse of the Ross Ice Shelf during the late
763 Holocene: Proceedings of the National Academy of Sciences, p. 201516908.

764 Zattin, M., Andreucci, B., Thomson, S. N., Reiners, P. W., and Talarico, F. M., 2012,
765 New constraints on the provenance of the ANDRILL AND-2A succession
766 (western Ross Sea, Antarctica) from apatite triple dating: Geochemistry
767 Geophysics Geosystems, v. 13.

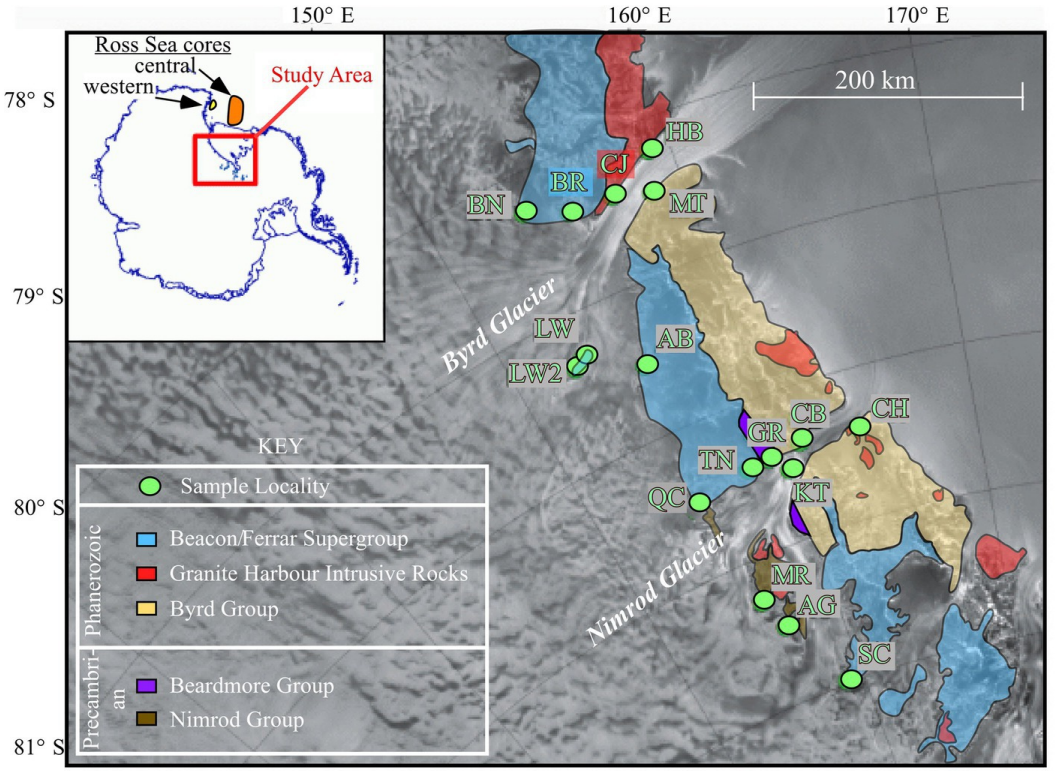
150° E
160° E
170° E
78° S
79° S
80° S
81° S
Ross Sea cores
central
western
Study Area
200 km
HB
CJ
BR
BN
MT
Byrd Glacier
LW
LW2
AB
CB
CH
GR
TN
KT
QC
Nimrod Glacier
MR
AG
SC
KEY
Sample Locality
Phanerozoic
Beacon/Ferrar Supergroup
Granite Harbour Intrusive Rocks
Byrd Group
Precambrian
Beardmore Group
Nimrod Group

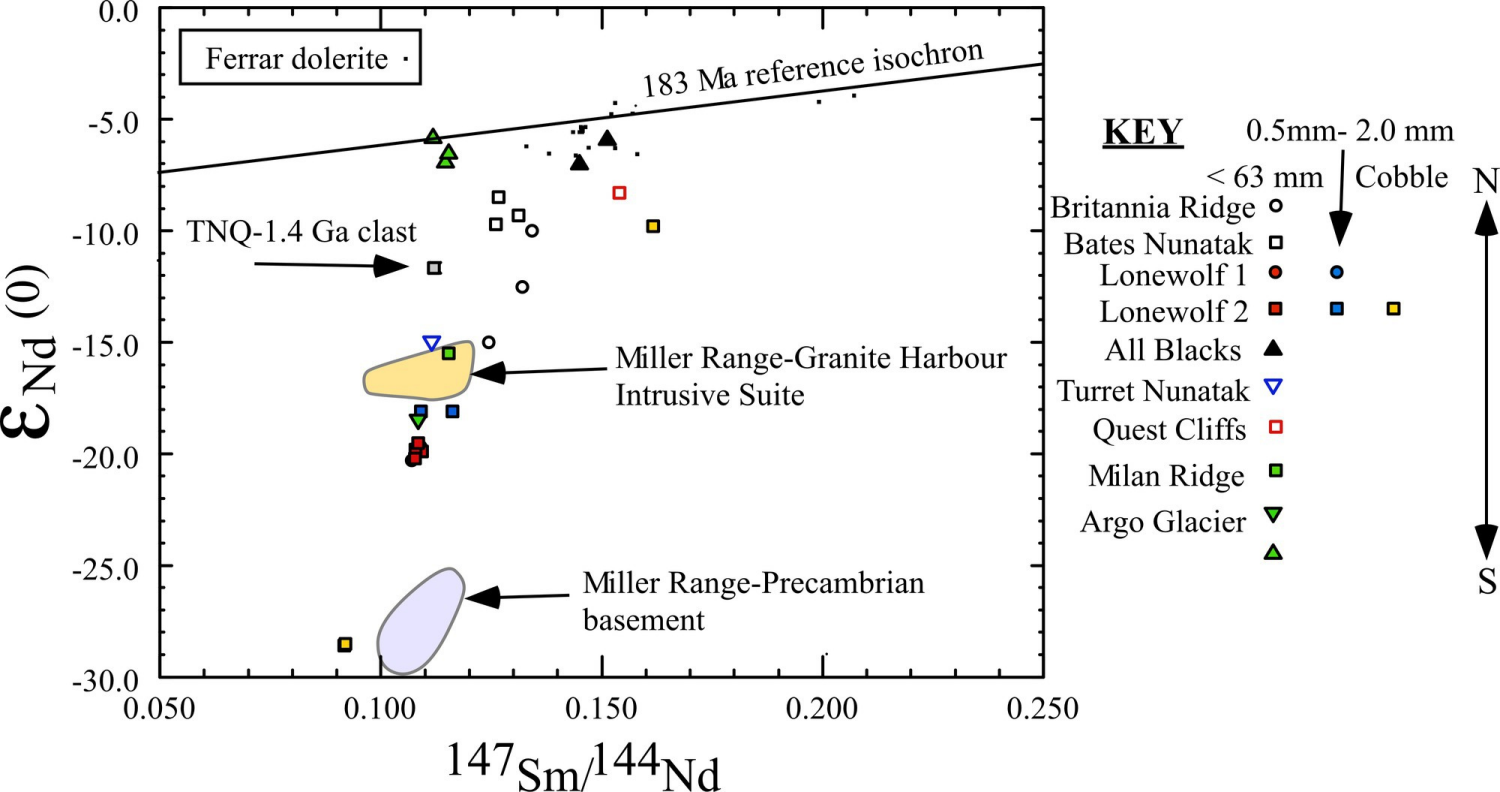
Ferrar dolerite
183 Ma reference isochron
TNQ-1.4 Ga clast
Miller Range-Granite Harbour Intrusive Suite
Miller Range-Precambrian basement
KEY
0.5mm- 2.0 mm
< 63 mm
Cobble
Britannia Ridge
Bates Nunatak
Lonewolf 1
Lonewolf 2
All Blacks
Turret Nunatak
Quest Cliffs
Milan Ridge
Argo Glacier
N
S
0.0
-5.0
-10.0
-15.0
-20.0
-25.0
-30.0
0.050
0.100
0.150
0.200
0.250
εNd (0)
147Sm/144Nd

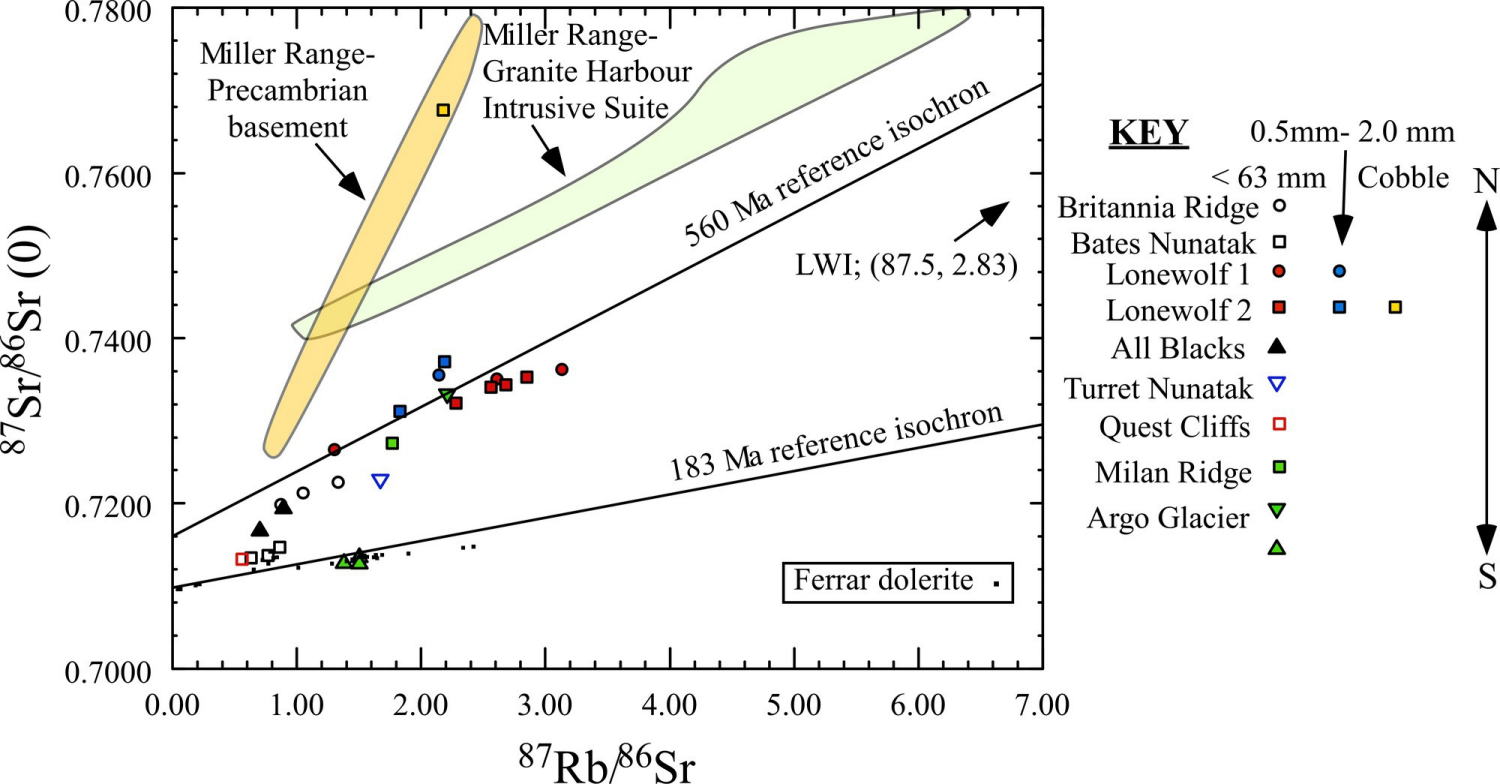
Miller Range-
Precambrian
basement
Miller Range-
Granite Harbour
Intrusive Suite
560 Ma reference isochron
LWI; (87.5, 2.83)
183 Ma reference isochron
Ferrar dolerite
KEY
0.5mm- 2.0 mm
< 63 mm
Cobble
Britannia Ridge
Bates Nunatak
Lonewolf 1
Lonewolf 2
All Blacks
Turret Nunatak
Quest Cliffs
Milan Ridge
Argo Glacier
N
S
0.7800
0.7600
0.7400
0.7200
0.7000
0.00
1.00
2.00
3.00
4.00
5.00
6.00
7.00
$^{87}Sr/^{86}Sr$ (0)
$^{87}Rb/^{86}Sr$

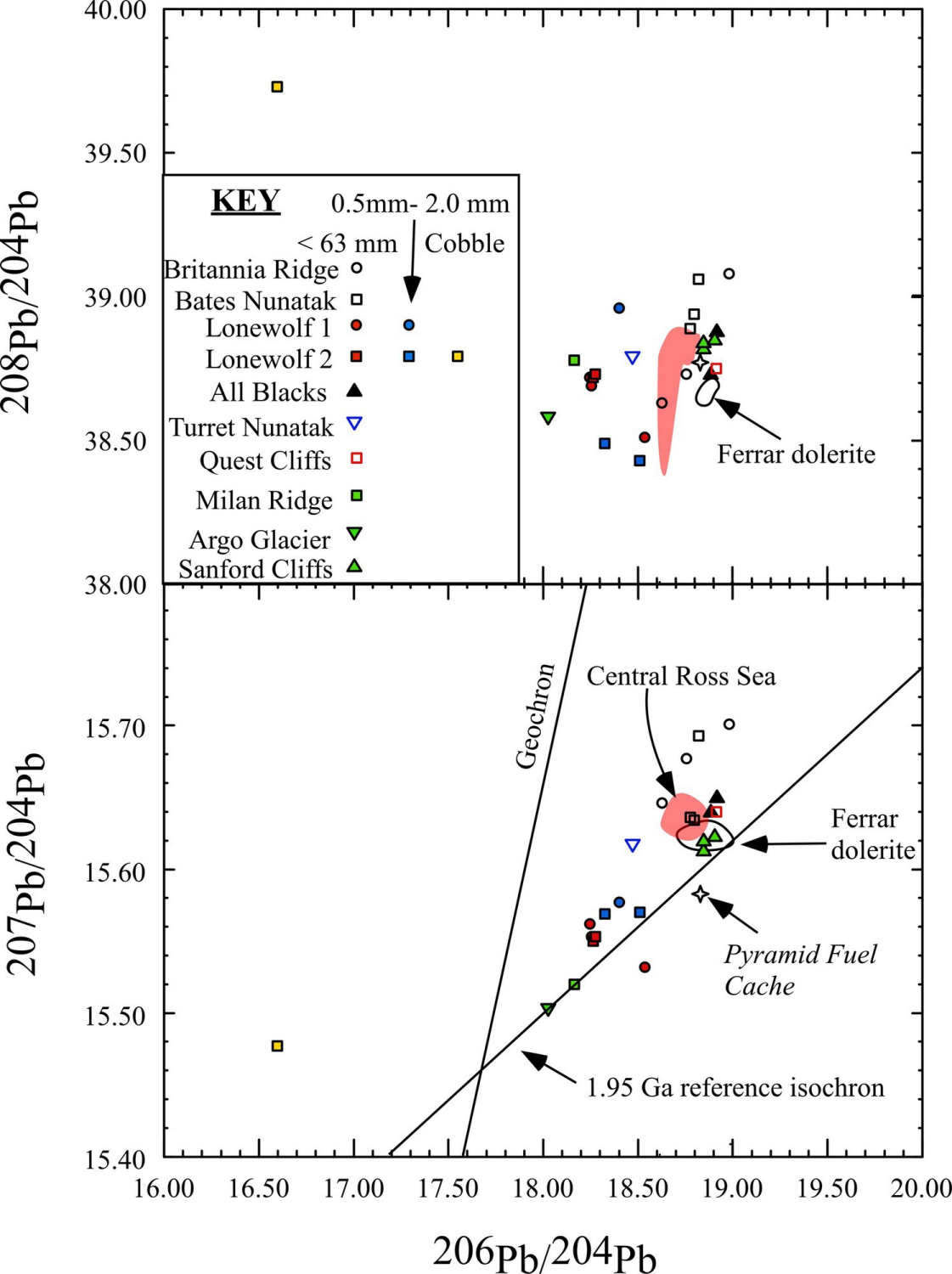
KEY
0.5mm- 2.0 mm
< 63 mm
Cobble
Britannia Ridge
Bates Nunatak
Lonewolf 1
Lonewolf 2
All Blacks
Turret Nunatak
Quest Cliffs
Milan Ridge
Argo Glacier
Sanford Cliffs
Ferrar dolerite
Geochron
Central Ross Sea
Ferrar dolerite
Pyramid Fuel Cache
1.95 Ga reference isochron
208Pb/204Pb
207Pb/204Pb
206Pb/204Pb
40.00
39.50
39.00
38.50
38.00
15.70
15.60
15.50
15.40
16.00
16.50
17.00
17.50
18.00
18.50
19.00
19.50
20.00

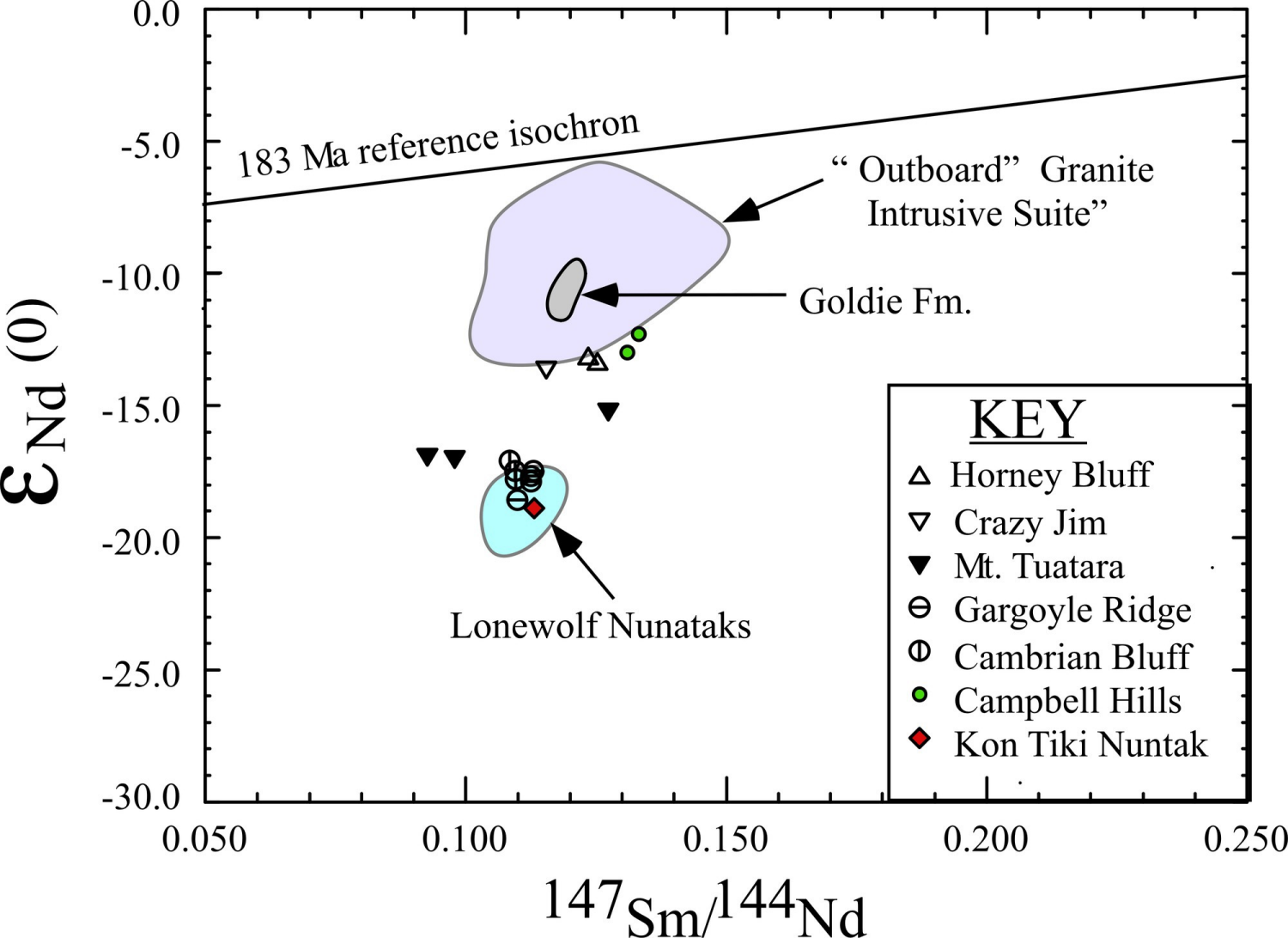
0.0
-5.0
-10.0
-15.0
-20.0
-25.0
-30.0
ε_{Nd} (0)
183 Ma reference isochron
" Outboard" Granite Intrusive Suite"
Goldie Fm.
Lonewolf Nunataks
KEY
Horney Bluff
Crazy Jim
Mt. Tuatara
Gargoyle Ridge
Cambrian Bluff
Campbell Hills
Kon Tiki Nuntak
0.050
0.100
0.150
0.200
0.250
$^{147}Sm/^{144}Nd$

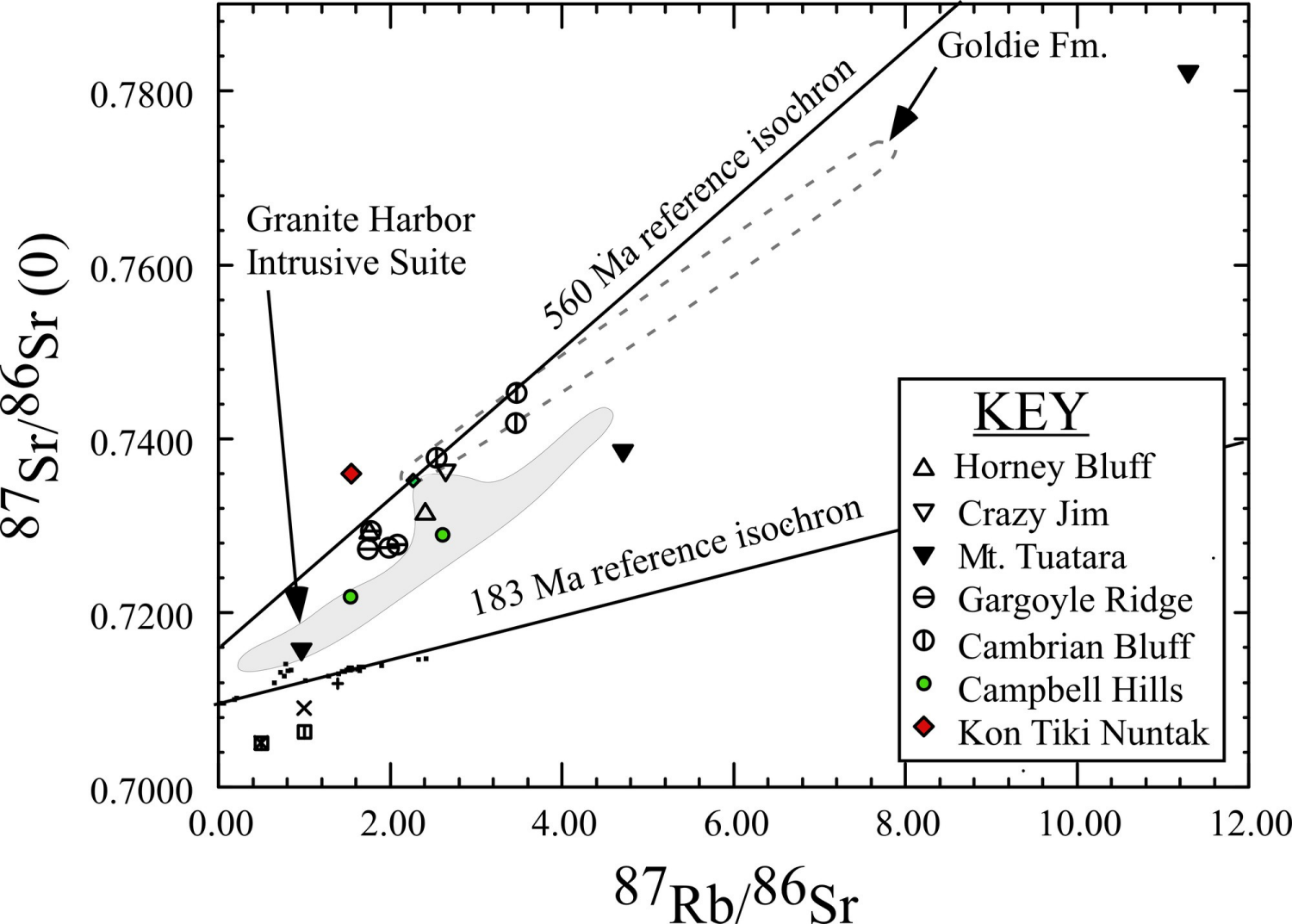
Goldie Fm.
560 Ma reference isochron
Granite Harbor
Intrusive Suite
183 Ma reference isochron
KEY
Horney Bluff
Crazy Jim
Mt. Tuatara
Gargoyle Ridge
Cambrian Bluff
Campbell Hills
Kon Tiki Nuntak
0.7800
0.7600
0.7400
0.7200
0.7000
0.00
2.00
4.00
6.00
8.00
10.00
12.00
$^{87}Sr/^{86}Sr$ (0)
$^{87}Rb/^{86}Sr$

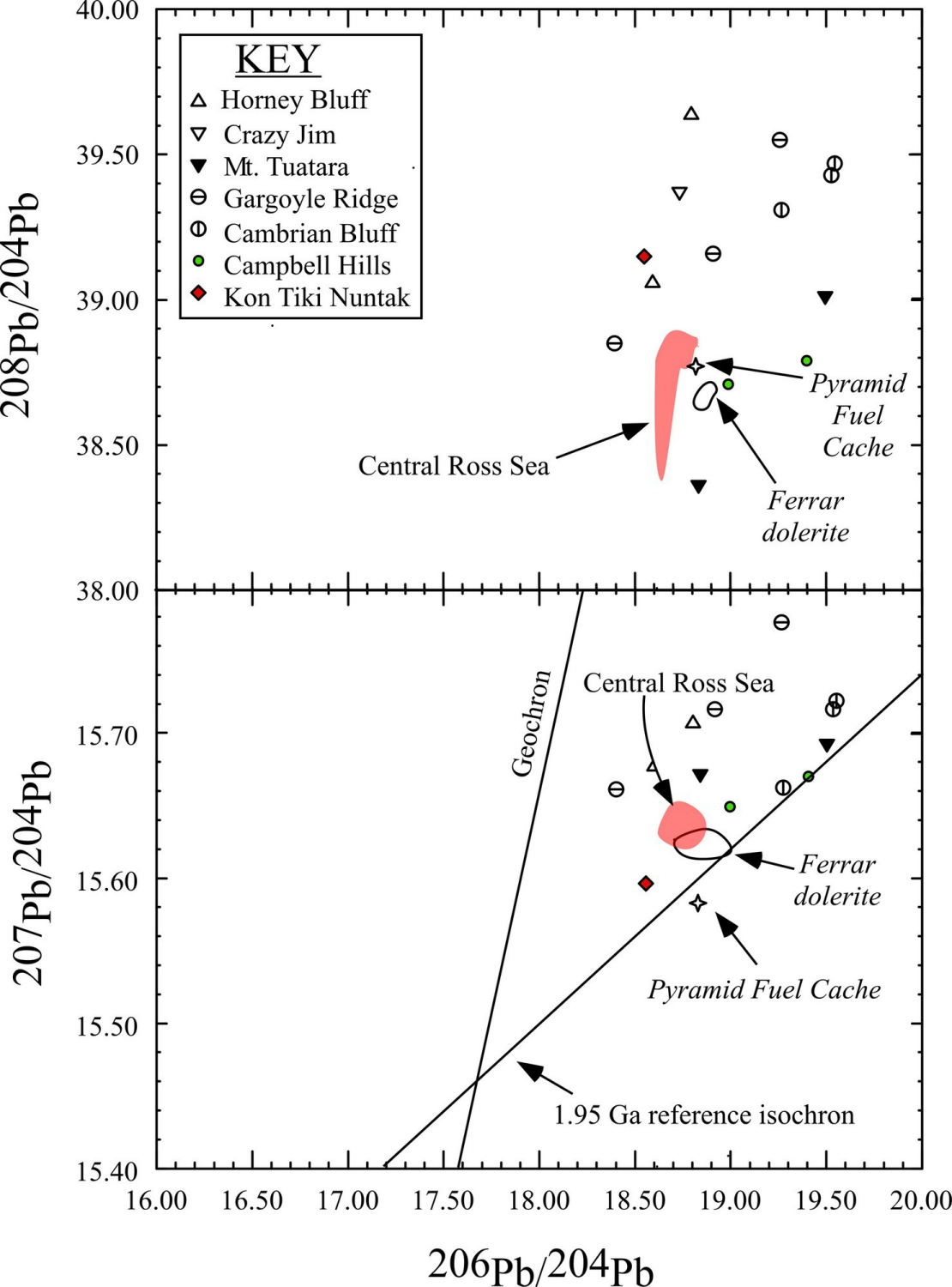
KEY
Horney Bluff
Crazy Jim
Mt. Tuatara
Gargoyle Ridge
Cambrian Bluff
Campbell Hills
Kon Tiki Nuntak
Central Ross Sea
Pyramid Fuel Cache
Ferrar dolerite
Geochron
1.95 Ga reference isochron
208Pb/204Pb
207Pb/204Pb
206Pb/204Pb
40.00
39.50
39.00
38.50
38.00
15.70
15.60
15.50
15.40
16.00
16.50
17.00
17.50
18.00
18.50
19.00
19.50
20.00

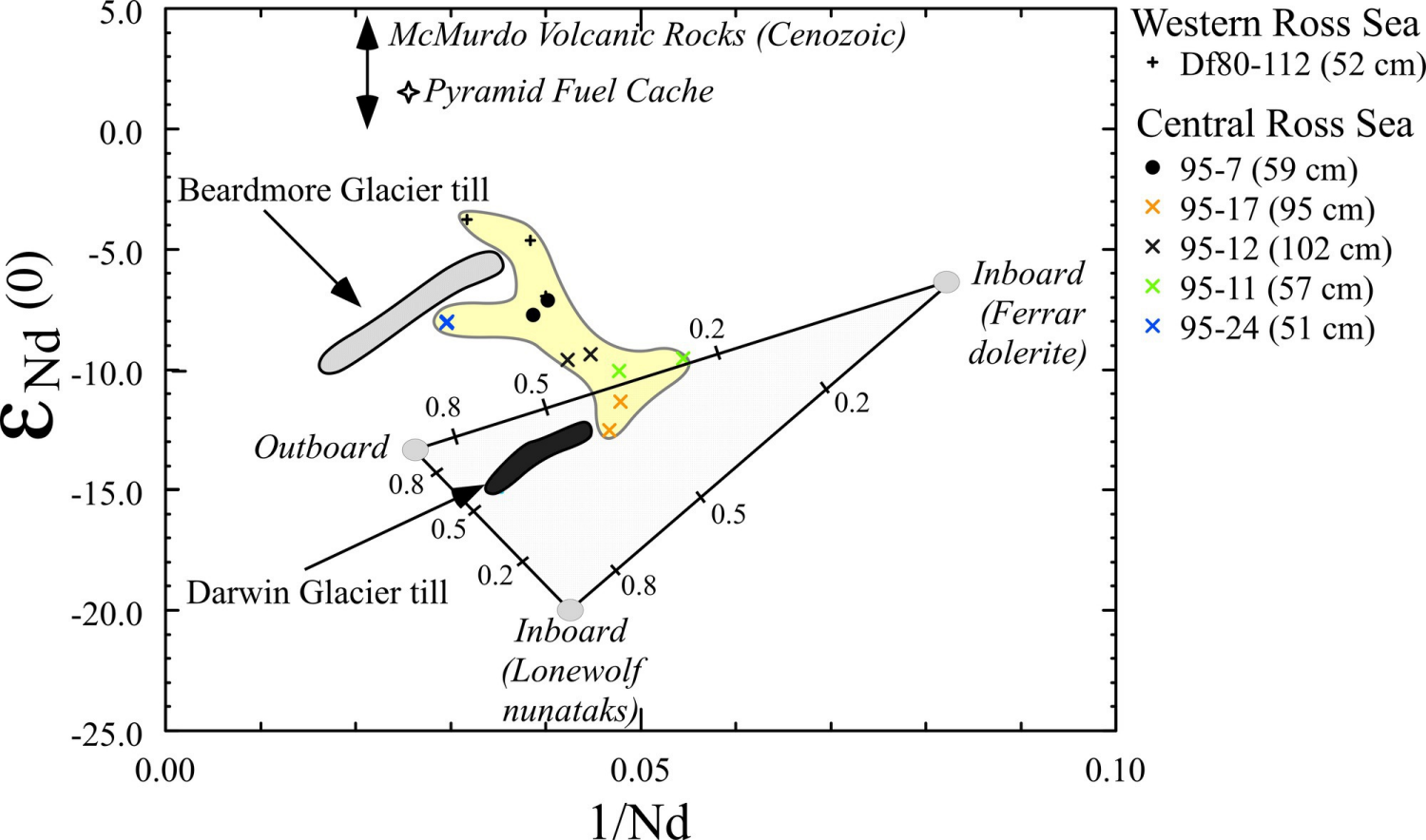
McMurdo Volcanic Rocks (Cenozoic)
Pyramid Fuel Cache
Beardmore Glacier till
Darwin Glacier till
Outboard
Inboard (Ferrar dolerite)
Inboard (Lonewolf nunataks)
0.2
0.5
0.8
εNd (0)
1/Nd
5.0
0.0
-5.0
-10.0
-15.0
-20.0
-25.0
0.00
0.05
0.10
Western Ross Sea
Df80-112 (52 cm)
Central Ross Sea
95-7 (59 cm)
95-17 (95 cm)
95-12 (102 cm)
95-11 (57 cm)
95-24 (51 cm)

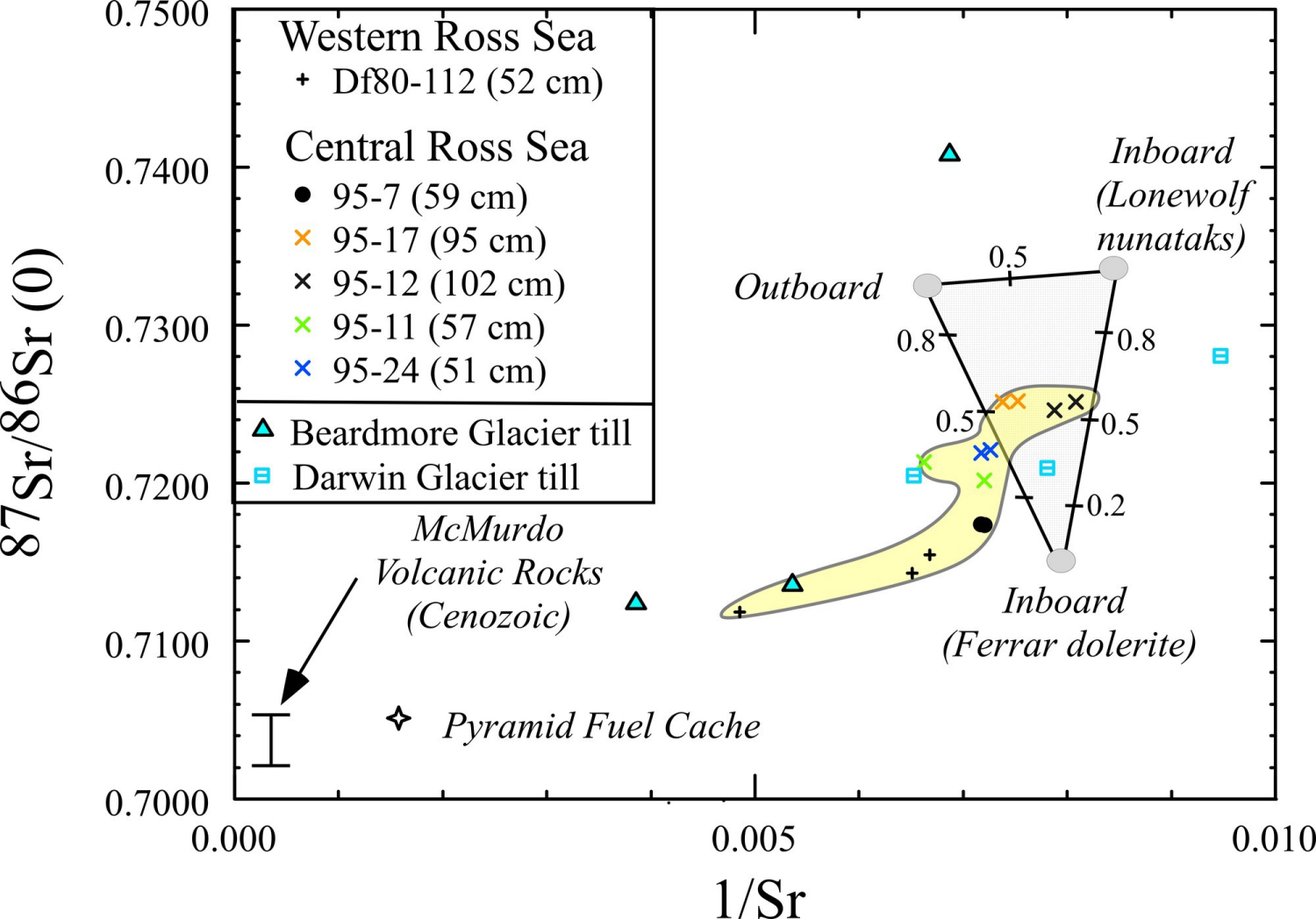
Western Ross Sea
Df80-112 (52 cm)
Central Ross Sea
95-7 (59 cm)
95-17 (95 cm)
95-12 (102 cm)
95-11 (57 cm)
95-24 (51 cm)
Beardmore Glacier till
Darwin Glacier till
McMurdo Volcanic Rocks (Cenozoic)
Pyramid Fuel Cache
Outboard
Inboard (Lonewolf nunataks)
Inboard (Ferrar dolerite)
0.5
0.8
0.8
0.5
0.5
0.2
0.7500
0.7400
0.7300
0.7200
0.7100
0.7000
0.000
0.005
0.010
87Sr/86Sr (0)
1/Sr

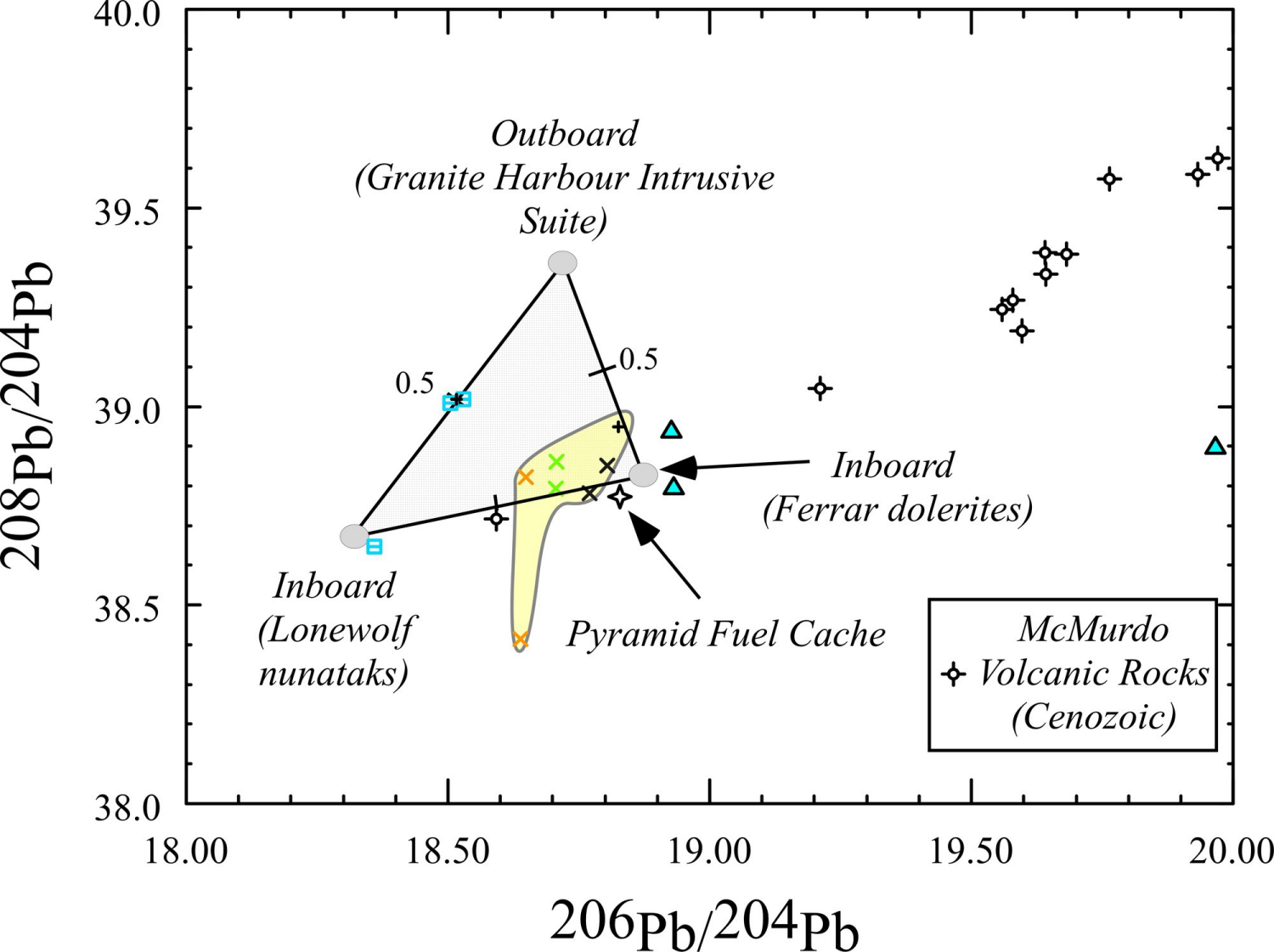
40.0
39.5
39.0
38.5
38.0
18.00
18.50
19.00
19.50
20.00
208Pb/204Pb
206Pb/204Pb
Outboard
(Granite Harbour Intrusive
Suite)
0.5
0.5
Inboard
(Ferrar dolerites)
Inboard
(Lonewolf
nunataks)
Pyramid Fuel Cache
McMurdo
Volcanic Rocks
(Cenozoic)

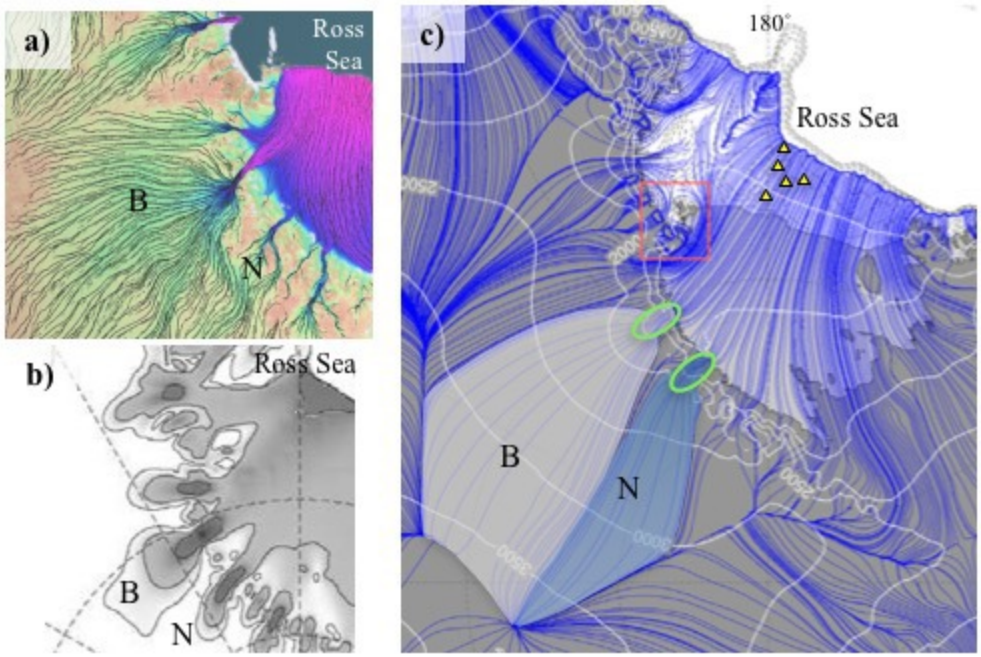
a)
Ross Sea
B
N
b)
Ross Sea
B
N
c)
180°
Ross Sea
B
N

Table 1. Nd, Sr and Pb isotopic compositions and isotope dilution trace element concentrations from Byrd and Nimrod glacial moraines

Sample	Location	Local Bedrock	Latitude	Longitude	Grain size	Rb(ppm)[2]	Sr (ppm)	$^{87}Rb/^{86}Sr$	$^{87}Sr/^{86}Sr(m)$[3]	Sm (ppm)	Nd (ppm)	$^{147}Sm/^{144}Nd$*	$^{143}Nd/^{144}Nd(m)$[3]	ε_{Nd} (0)[4]	T_{DM} (Ga)	$^{208}Pb/^{204}Pb$[5]	$^{207}Pb/^{206}Pb$	$^{206}Pb/^{204}Pb$
Byrd Glacier																		
1571	Britannia Ridge	Beacon/Ferrar	-80.3860	155.3330	<63µ	44	146	0.87	0.719879 ± 10	3.22	14.5	0.1342	0.512125 ± 11	-10.0	1.8	38.63	15.646	18.627
1572	*(BR)*	Supergroup			<63µ	44	120	1.05	0.721233 ± 10	3.03	13.9	0.1320	0.511999 ± 16	-12.5	1.9	38.73	15.677	18.756
1573	"				<63µ	50	108	1.33	0.722589 ± 14	3.68	17.9	0.1244	0.511871 ± 35	-15.0	2.0	39.08	15.701	18.980
1574	Bates Nunatak	Beacon/Ferrar	-80.2620	153.6530	<63µ	34	116	0.86	0.714667 ± 15	2.43	11.7	0.1261	0.512141 ± 31	-9.7	1.6	39.06	15.693	18.821
1575	*(BN)*	Supergroup			<63µ	25	94	0.77	0.713713 ± 14	1.94	8.9	0.1311	0.51216 ± 13	-9.3	1.6	38.89	15.636	18.775
1576	"				<63µ	29	132	0.63	0.713376 ± 10	2.26	10.8	0.1267	0.512204 ± 11	-8.5	1.5	38.94	15.634	18.796
1588	Horney Bluff	Granite Harbor Igneous Suite	-80.2090	159.1430	<63µ	93	152	1.76	0.729311 ± 7	7.96	39.1	0.1232	0.511961 ± 6	-13.2	1.8	39.64	15.708	18.806
1589	*(HB)*				<63µ	120	143	2.41	0.731504 ± 13	6.01	29.1	0.1250	0.511951 ± 7	-13.4	1.9	39.06	15.678	18.603
1618	Crazy Jim *(CJ)*	Granite Harbor Igneous Suite	-80.4020	157.1340	<63µ	145	158	2.65	0.736235 ± 10	8.64	45.4	0.1152	0.511941 ± 5	-13.6	1.7	39.37	15.624	18.743
1577	Lonewolf 1	Beacon/Ferrar Supergroup	-81.3000	153.1670	<63µ	94	209	1.30	0.726510 ± 10	4.94	28.0	0.1070	0.511597 ± 9	-20.3	2.1	38.72	15.562	18.247
1577	*(LW 1)*				0.5mm-2mm	57	78	2.14	0.735497 ± 10	2.62	14.5	0.1090	0.511627 ± 7	-19.7	2.1	38.96	15.577	18.402
1578	"				<63µ	103	95	3.13	0.736255 ± 11	3.57	20.1	0.1076	0.511602 ± 5	-20.2	2.1	38.51	15.532	18.535
1579	"				<63µ	91	101	2.61	0.735074 ± 11	4.00	22.4	0.1082	0.511626 ± 11	-19.7	2.0	38.69	15.553	18.254
1580	Lonewolf 2	Beacon/Ferrar Supergroup	-81.3410	152.6790	<63µ	88	111	2.28	0.732129 ± 10	3.90	21.6	0.1093	0.511619 ± 7	-19.9	2.1	38.72	15.550	18.264
1580	*(LW 2)*				0.5mm-2mm	55	87	1.83	0.731134 ± 23	2.01	10.5	0.1162	0.511709 ± 11	-18.1	2.1	38.43	15.570	18.511
1581	"				<63µ	96	104	2.68	0.734337 ± 12	4.17	23.4	0.1079	0.511621 ± 7	-19.8	2.0	-	-	-
1582	"				<63µ	95	107	2.56	0.734045 ± 11	4.31	24.2	0.1078	0.511605 ± 9	-20.2	2.1	-	-	-
1582	"				0.5mm-2mm	55	72	2.19	0.737178 ± 19	2.07	11.5	0.1090	0.511710 ± 10	-18.1	1.9	38.49	15.569	18.325
1583	"				<63µ	98	100	2.85	0.735296 ± 12	4.18	23.3	0.1084	0.511636 ± 6	-19.5	2.0	38.73	15.553	18.274
LWE	"				cobble	135	179	2.18	0.767606 ± 12	4.63	30.5	0.0918	0.511172 ± 8	-28.6	2.3	39.73	15.477	16.596
LWI	"				cobble	339	11	87.5	2.827513 ± 53	3.91	14.6	0.1616	0.512134 ± 8	-9.8	2.7	-	-	-
1584	All Blacks	Beacon/Ferrar Supergroup	-81.5219	155.5271	<63µ	29	120	0.70	0.716820 ± 11	2.58	10.8	0.1450	0.512281 ± 11	-7.0	1.7	38.88	15.650	18.917
1585	*(AB)*	*(Ferrar dolerites)*			<63µ	30	98	0.89	0.719519 ± 15	1.51	6.1	0.1512	0.512337 ± 10	-5.9	1.7	38.73	15.640	18.885
1590	Mt. Tuatara	Byrd Group	-80.4780	158.6700	<63µ	13	37	0.97	0.715736 ± 19	0.52	2.45	0.1271	0.511858 ± 15	-15.2	2.1	38.36	15.672	18.844
1591	*(MT)*	*(Shackleton Ls.)*			<63µ	14	9	4.71	0.738534 ± 16	0.28	1.76	0.0976	0.511766 ± 13	-17.0	1.7	-	-	-
1592	"				<63µ	20	5	11.3	0.782125 ± 23	0.32	2.10	0.0923	0.511771 ± 21	-16.9	1.6	39.01	15.693	19.505
Nimrod Glacier																		
1593	Sanford Cliffs	Beacon/Ferrar Supergroup	-83.9785	158.9004	<63µ	68	141	1.38	0.712819 ± 13	3.38	17.9	0.1146	0.512285 ± 7	-6.9	1.2	38.82	15.613	18.847
1594	*(SC)*				<63µ	70	135	1.50	0.713524 ± 14	3.26	17.1	0.1153	0.512305 ± 26	-6.5	1.1	38.84	15.620	18.845
1595	"				<63µ	70	136	1.50	0.712777 ± 13	3.19	17.3	0.1118	0.512343 ± 8	-5.8	1.0	38.85	15.623	18.905
1596	Gargoyle Ridge	Beardmore	-82.4150	159.2927	<63µ	95	138	1.99	0.727497 ± 15	4.06	21.9	0.1123	0.511729 ± 14	-17.7	2.0	-	-	-
1597	(GR)	*(Goldie Fm.)*			<63µ	94	156	1.74	0.727364 ± 11	4.27	23.0	0.1122	0.511721 ± 37	-17.9	2.0	39.16	15.717	18.919
1598	"				<63µ	106	147	2.08	0.727826 ± 15	4.45	23.9	0.1127	0.511739 ± 8	-17.5	2.0	39.55	15.777	19.268
1599	"				<63µ	91	147	1.78	0.729450 ± 5	4.08	22.5	0.1097	0.511683 ± 8	-18.6	0.6	38.85	15.662	18.405
1600	Cambrian Bluff	Byrd Group	-82.3778	161.0307	<63µ	62	51	3.47	0.745329 ± 15	1.44	7.99	0.1092	0.511743 ± 12	-17.5	1.9	39.31	15.663	19.277
1601	*(CB)*	*(Starshot Fm.)*			<63µ	41	46	2.54	0.737831 ± 14	1.22	6.84	0.1082	0.511759 ± 7	-17.1	1.9	39.47	15.723	19.556
1602	"				<63µ	56	46	3.46	0.741861 ± 11	1.40	7.76	0.1093	0.511724 ± 27	-17.8	1.9	39.43	15.717	19.537
1605	Campbell Hills	Byrd Group	-82.4021	163.9743	<63µ	143	269	1.54	0.721877 ± 13	5.25	24.3	0.1307	0.511974 ± 8	-13.0	2.0	38.71	15.650	19.000
1606	*(CH)*	*(Starshot Fm.)*			<63µ	207	229	2.61	0.728964 ± 9	6.26	28.5	0.1329	0.512007 ± 16	-12.3	2.0	38.79	15.671	19.410
1607	Turret Nunatak*(TN)*	Beacon/Ferrar Supergroup	-82.4324	158.1207	<63µ	75	129	1.67	0.722830 ± 14	3.26	17.7	0.1115	0.511869 ± 20	-15.0	1.7	38.79	15.617	18.471
1611	Argo Glacier *(AG)*	Nimrod Group	-83.4953	156.7412	<63µ	86	112	2.21	0.733107 ± 11	4.19	23.4	0.1085	0.511689 ± 10	-18.5	2.0	38.58	15.503	18.027
1613	Quest Cliffs *(QC)*	Beacon/Ferrar Supergroup	-82.5394	154.8313	<63µ	24	121	0.56	0.713201 ± 12	1.85	7.26	0.1541	0.512214 ± 8	-8.3	2.1	38.75	15.640	18.913
1615	Milan Ridge *(MR)*	Nimrod Group	-83.2831	156.0373	<63µ	85	139	1.77	0.727253 ± 12	4.55	23.9	0.1154	0.511841 ± 8	-15.5	1.9	38.78	15.520	18.164
1619	Kon Tiki Nuntak *(KT)*	Beardmore *(Goldie Fm.)*	-82.5308	160.0893	<63µ	87	163	1.55	0.735999 ± 13	6.57	35.2	0.1129	0.511670 ± 5	-18.9	2.1	39.15	15.597	18.560

[2] Isotope dilution concentration determinations accurate to ~1% for Rb and Sr, and 0.5% for Sm and Nd. Total procedural blanks averaged ~1ng for Pb and Sr, and 100pg for Nd, during study period.

[3] Measured $^{87}Sr/^{86}Sr$ ratios were analyzed using four-collector static mode measurements. Thirty measurements of SRM-987 during study period yielded mean $^{87}Sr/^{86}Sr$=0.71032+/- 2. Those analyses in bold were corrected to SRM-987 value of 0.71028.

Measured $^{143}Nd/^{144}Nd$ normalized to $^{146}Nd/^{144}Nd$=0.7219. Analyses were dynamic mode, three-collector measurements. Thirty-three measurements of the La Jolla Nd standard during the study period yielded a mean $^{143}Nd/^{144}Nd$=0.511838+/-8 (2-σ mean).

[5] ε_{Nd} values calculated using a present-day $^{143}Nd/^{144}Nd$ (CHUR)=0.512638

[6] Pb isotopic analyses were four-collector static mode measurements. Sixteen measurements of SRM-981 during the study period yielded $^{208}Pb/^{204}Pb$=36.56 +/- 0.03, $^{207}Pb/^{204}Pb$=15.449+/-0.008, $^{206}Pb/^{204}Pb$=16.905+/-0.007 (2-σ mean). Measured Pb isotope ratios were corrected to SRM-981 values ($^{208}Pb/^{204}Pb$=36.721, $^{207}Pb/^{204}Pb$=15.491, $^{206}Pb/^{204}Pb$=16.937).